The Mechanism of Inward Rectification of Potassium Channels: "Long-pore Plugging" by Cytoplasmic Polyamines

A. N. LOPATIN, E. N. MAKHINA, and C. G. NICHOLS

From the Department of Cell Biology and Physiology, Washington University School of Medicine, St. Louis, Missouri 63110

ABSTRACT The mechanism of inward rectification was examined in cell-attached and inside-out membrane patches from *Xenopus* oocytes expressing the cloned strong inward rectifier HRK1. Little or no outward current was measured in cell-attached patches. Inward currents reach their maximal value in two steps: an instantaneous phase followed by a time-dependent "activation" phase, requiring at least two exponentials to fit the time-dependent phase. After an activating pulse, the quasi-steady state current-voltage (*I-V*) relationship could be fit with a single Boltzmann equation (apparent gating charge, $Z = 2.0 \pm 0.1$, $n = 3$). Strong rectification and time-dependent activation were initially maintained after patch excision into high $[K^+]$ (K-INT) solution containing 1 mM EDTA, but disappeared gradually, until only a partial, slow inactivation of outward current remained. Biochemical characterization (Lopatin, A. N., E. N. Makhina, and C. G. Nichols. 1994. *Nature.* 372:366–396.) suggests that the active factors are naturally occurring polyamines (putrescine, spermidine, and spermine). Each polyamine causes reversible, steeply voltage-dependent rectification of HRK1 channels. Both the blocking affinity and the voltage sensitivity increased as the charge on the polyamine increased. The sum two Boltzmann functions is required to fit the spermine and spermidine steady state block. Putrescine unblock, like Mg^{2+} unblock, is almost instantaneous, whereas the spermine and spermidine unblocks are time dependent. Spermine and spermidine unblocks (current activation) can each be fit with single exponential functions. Time constants of unblock change *e*-fold every 15.0 ± 0.7 mV ($n = 3$) and 33.3 ± 6.4 mV ($n = 5$) for spermine and spermidine, respectively, matching the voltage sensitivity of the two time constants required to fit the activation phase in cell-attached patches. It is concluded that inward rectification in intact cells can be entirely accounted for by channel block. Putrescine and Mg^{2+} ions can account for instantaneous rectification; spermine and spermidine provide a slower rectification corresponding to so-called intrinsic gating of inward rectifier K channels. The structure of spermine and spermidine leads us to suggest a specific model in which the pore of the inward rectifier channel is plugged by polyamines that enter deeply into the pore and bind at sites within the membrane field. We propose a model that takes into account the linear structure of the natural polyamines and electrostatic repulsion between two molecules inside the pore. Experimentally observed instantaneous and steady state rectification of HRK1 channels as well as the time-dependent behavior of

J. GEN. PHYSIOL. © The Rockefeller University Press · 0022-1295/95/11/923/33 $2.00
Volume 106 November 1995 923–955

HRK1 currents are then well fit with the same set of parameters for all tested voltages and concentrations of spermine and spermidine.

INTRODUCTION

Many membrane currents show changes of conductance with voltage, a property termed rectification. The physiological roles of potassium (K) currents are critically dependent on their rectifying properties, and K currents have been classified into two major groups on this basis (Hille, 1992). Outward or delayed rectifiers are primarily responsible for modulation of action potential shape; outward rectification results from time-dependent closure of the channel at negative voltages owing to conformational changes involving charged membrane spanning domains (Liman, Hess, Weaver, and Koren, 1991; Lopez, Jan, and Jan, 1991). Inward rectifier K^+ (Kir) channels (Katz, 1949; Noble, 1965) are open at hyperpolarized membrane potentials, and K^+ conductance decreases with depolarization. Classically described strong inward rectification is so strong that very little current flows positive to the potassium reversal potential (E_K). Inward rectification was first termed "anomalous rectification" (Katz, 1949), because it is opposite to what is expected from the K^+ gradient and opposite to the effect of voltage on delayed, or outward, rectifier K currents. Inward rectification has been described in numerous cell types (Hille, 1992). In the heart, for example, it is an essential property allowing maintenance of a stable resting potential without short circuiting the long action potentials that are necessary for normal excitation and relaxation cycles (Weidmann, 1951; Hille, 1992). Other proposed roles for inward rectifiers are in determination of cell resting potential, modulation of excitability, and buffering of extracellular K^+ in various neuronal and nonneuronal tissues (Kandel and Tauc, 1966; Hagiwara and Takahashi, 1974; Constanti and Galvan, 1983; Newman, 1985, 1993; Brew, Gray, Mobbs, and Attwell, 1986; Hestrin, 1987; Brismar and Collins, 1989).

Work on native channels has demonstrated that a voltage-dependent block by Mg^{2+} ions contributes to strong inward rectification (Matsuda, Saigusa, and Irisawa, 1987; Vandenberg, 1987), but an apparently intrinsic gating, dependent on both E_K and membrane potential, seems to provide the very steep rectification that characterizes these channels (Hagiwara, Miyazaki, and Rosenthal, 1976; Stanfield, Standen, Leech, and Ashcroft, 1981; Carmeliet, 1982; Kurachi, 1985; Matsuda et al., 1987; Tourneur, Mitra, Morad, and Rougier, 1987; Ishihara, Mitsuiye, Noma, and Takano, 1989; Oliva, Cohen, and Pennefather, 1990). We have recently provided evidence that intrinsic gating actually requires soluble cytoplasmic factors and that these factors may be naturally occurring cytoplasmic polyamines (van Leeuwenhoek, 1678; Bachrach, 1973; Lopatin, Makhina and Nichols, 1994; Seiler, 1994). In this paper, we show that the phenomenologically described processes of time-dependent "activation" of inward current and "intrinsic" gating represents the unblock and block of the channel pore by intracellular polyamines. The results lead us to suggest that the long pore of the inward rectifier channel (Hille and Schwartz, 1978; Hille, 1992) is essentially plugged by the linear polyamines entering deeply into it. We examine potential kinetic schemes and demonstrate how one

specific model can explain the kinetics of polyamine action, and hence intrinsic rectification, in Kir channels. The known three-dimensional structure of polyamine molecules should allow them to be used as a probe for the structure of the channel pore. The electrochemical model that can explain polyamine action implies structural consequences of polyamine block and provides an estimation of the real dimensions of the conduction pathway of strong inward rectifiers.

METHODS

Oocyte Expression of Kir Channels

cDNAs were propagated in the transcription-competent vector pBluescript SK− in *Escherichia coli* TG1. Capped cRNAs were transcribed in vitro from linearized cDNAs using T7 RNA polymerase. Stage V–VI *Xenopus* oocytes were isolated by partial ovariectomy under tricaine anesthesia and then defolliculated by treatment with 1 mg/ml collagenase (type 1A; Sigma Chemical Co., St. Louis, MO) in zero Ca^{2+} ND96 (see below) for 1 h. 2 to 24 h after defolliculation, oocytes were pressure injected with ~50 nl of 1–100 ng/μl cRNA. Oocytes were kept in ND96 + 1.8 mM Ca^{2+} (see below), supplemented with penicillin (100 U/ml) and streptomycin (100 μg/ml) for 1–7 days before experimentation.

Electrophysiology

Oocytes were placed in hypertonic solution (in mM: KCl, 60; EGTA, 10; HEPES, 40; sucrose, 250; $MgCl_2$, 8; pH 7.0) for 5–30 min to shrink the oocyte membrane from the vitelline membrane. The vitelline membrane was removed from the oocyte using Dumont No. 5 forceps. Oocyte membranes were patch clamped using an Axopatch 1B patch clamp apparatus (Axon Instruments Inc., Foster City, CA). Fire-polished micropipettes were pulled from thin-walled glass (WPI Inc., New Haven, CT) on a horizontal puller (Sutter Instrument Co., Novato, CA). Electrode resistance was typically 0.5–2 MΩ when filled with K-INT solution (see below) with tip diameters of 2–20 μm. Pipette capacitance was minimized by coating them with a mixture of Parafilm (American National Can Co., Greenwich, CT) and mineral oil. Experiments were performed at room temperature in a chamber mounted on the stage of an inverted microscope (Nikon Diaphot; Nikon Inc., Garden City, NY). PClamp software (Axon Inst. Inc)and a Labmaster TL125 D/A converter were used to generate voltage pulses. Data were normally filtered at 5 kHz, and signals were digitized at 22 kHz (Neurocorder; Neuro Data Instruments Corp., New York, NY) and stored on video tape. Data could then be redigitized into a microcomputer using Axotape (Axon Instruments Inc.). Alternatively, signals were digitized on-line using PClamp and stored on disk for off-line analysis. Where necessary, currents were corrected for linear leak using a P/4 voltage protocol with +50 mV conditional prepulse. In most cases, especially with inside-out patches and low concentrations of polyamines or Mg^{2+}, leak current and capacity transients were corrected off line with the P/1 procedure (+50 mV or higher conditional prepulse). In most experiments, the bath and pipette solutions were standard high $[K^+]$ extracellular solution (K-INT) containing (mM): 140 KCl; 10 HEPES; 1 K-EGTA; pH 7.35 (with KOH). The bath solution additionally typically contained 1 mM K-EDTA.

Analysis

Wherever possible, data are presented as means ± SE (standard error). Microsoft Solver (Microsoft Corp., Redmond, WA) was used to fit data by a least-square algorithm. Quasi-steady state current-voltage (I-V) relationships were measured as follows: voltage steps were applied from 0

mV holding potential to −80 mV to "activate" current, and then currents at the end of subsequent test pulses (usually 5 ms) were measured. True steady state I-V relationships were obtained by fitting current traces in response to test pulses with an exponential function: $A \cdot \exp(-t/\tau) + B$, where t is time, and A, B, and τ are constants. Instantaneous I-V relationships were obtained by extrapolation of the fitted exponential function to the beginning of the test pulse. The "activation" of inward currents was fitted with the following function: $A \cdot \exp(-t/\tau_I) \cdot [1 - \exp(-t/\tau)] + B$, where τ corresponds to the time constant of inward current activation, and τ_I represents a modulation function to describe the inactivation at extreme negative membrane potentials. In some on-cell patches, an additional exponential term was included (see Results). The inactivation of outward currents was usually estimated by a single exponential approximation, with the steady state level taken as a free parameter ($I = A \cdot \exp(-t/\tau) + B$).

Modeling of Polyamine-induced Kinetics

Programs describing the kinetic schemes were written in Turbo Pascal (Borland International Inc., Scotts Valley, CA). The system of first-order differential equations describing a given kinetic scheme was numerically integrated and compared with real experimental currents. Adjustable parameters were varied to obtain the best fit with the whole set of current records. At any given membrane potential, rate constants could differ by more than six orders of magnitude, and commercially available integration programs (e.g., MathCad for Windows, fourth-order Runge-Kutter method) were not suitable. Therefore, fast and slow transitions were treated separately: slow transitions were integrated with a first-order Runge–Kutter method, and fast transitions were calculated at the same time as steady state data using algebraic solutions to provide results in acceptable time. Since rate constants are dependent on voltage and change by many orders in magnitude with a change in membrane potential, the program was designed to automatically switch between numeric integration and algebraic calculation depending on the membrane potential.

RESULTS

'Intrinsic' Gating of HRK1 Channel Currents in Cell-attached Patches

To examine the mechanism of inward rectification, we expressed cloned strong inward rectifier HRK1 channels (Makhina, Kelly, Lopatin, Mercer, and Nichols, 1994; Perier, Radeke, and Vandenberg, 1994) in *Xenopus* oocytes. Because of the high level of HRK1 expression, inward currents of up to several nanoamperes could be measured in cell-attached membrane patches with 140 mM KCl in the pipette solution. After a voltage step to negative potentials, the amplitude of inward HRK1 currents increased approximately linearly with membrane potential, but little or no outward current was measured (Makhina et al., 1994). On a slow time scale, significant decay of inward current occurred (Fig. 1 *A*). The only cation in the pipette solution was potassium, making it unlikely that block of the current by nonpermeant cations was responsible. The rate and extent of current decay varied from patch to patch but was not obviously dependent on patch variables (pipette tip diameter, patch recess depth, current density), making it unlikely that such an effect was an artefact of external $[K^+]$ depletion or voltage-clamp limitations. This effect complicated true steady state measurement of inward currents, and to minimize contribution of current decay to the desired measurements, patch voltage was normally held at −20 or 0 mV, and was only stepped briefly (< 5 ms) to more negative voltages (−80 to −100 mV) for activation of the HRK1 current. On a faster

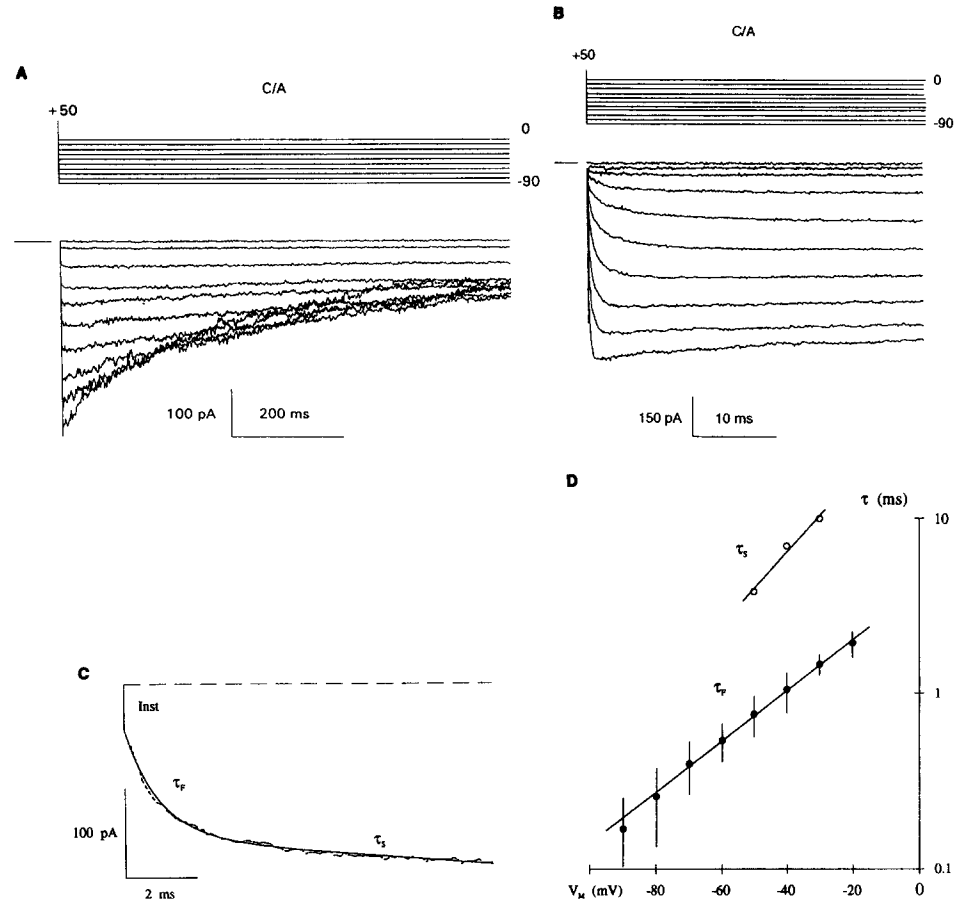

FIGURE 1. (*A*) Slow time-base records of cell-attached (C/A) HRK1 current in response to voltage steps from +50 mV to voltages between −90 and 0 mV. The pulse protocol is indicated above the record, and zero current is indicated by the horizontal dash. Interpulse duration was 3 s. (*B*) Fast time-base records of (C/A) HRK1 currents in response to voltage steps from +50 mV to voltages between −90 and 0 mV. (*C*) Time course of HRK1 current activation (*dashed*) after a step from +50 mV to −40 mV. The time-dependent activation is fitted by the sum of two exponentials (*solid*) with time constants τ_F = 1.1 ms and τ_S = 7.0 ms for this particular experiment, and an instantaneous (*Inst*) component. (*D*) Voltage dependence of the time constants for HRK1 "activation" in cell-attached patches. Each curve is a single exponential fit to the points. Data for τ_F are averaged from three experiments. Data for τ_S are taken from the experiment in (*B*).

time scale (Fig. 1 *B*), it is apparent that inward currents reach their maximal value in two steps, an instantaneous phase followed by a fast but clearly resolvable increase in amplitude up to the final value. Since the original discovery of inward rectification, this time-dependent increase in inward current has been referred to as "activation" (Hagiwara et al., 1976; Stanfield et al., 1981; Kurachi, 1985; Ishihara et al., 1989; Oliva et al., 1990). The activation phase of the current after a hyperpolar-

izing voltage step follows a complex time course. In addition to an instantaneous phase, at least two exponentials may be necessary to fit the observed time-dependent currents (Fig. 1 *C*), and each time constant shows marked voltage dependence (Fig. 1 *D*). The time constant of the fast component (τ_F) increased e-fold every 31.6 ± 2.8 mV ($n = 5$). The amplitude of the slow component was generally small compared with the fast component and could only be reliably measured in a narrow

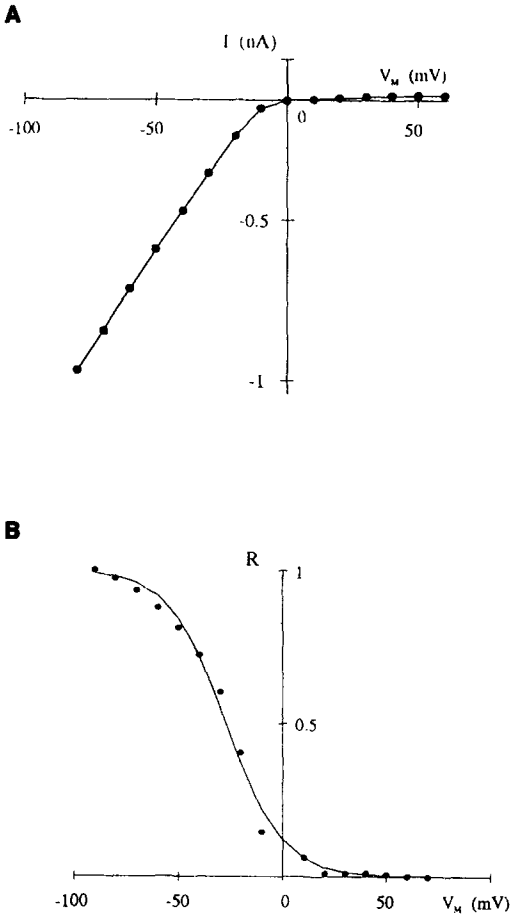

FIGURE 2. (*A*) Representative quasi-steady state current-voltage (I-V) relationship (see Methods) for HRK1 currents in cell-attached patches. Solid line is drawn by eye. (*B*) Currents in *A*, normalized to a linear approximation of the conductance by extrapolation from currents below −50 mV (R), plotted versus membrane potential (V_m). The data points are fitted with a single Boltzmann equation (see text).

voltage range (Fig. 1 *D*). For the most reliable single experiment, the estimated time constant of the slow component (τ_S) increased e-fold every 22 mV.

After a brief activating pulse to −80 or −100 mV, the quasi-steady state current-voltage (I-V) relationship was measured by depolarizing pulses (Fig. 2 *A*). It is apparent (Fig. 2 *B*) that the steady state HRK1 I-V relationship is steep. A single Boltzmann fit to the conductance-voltage relationship (Fig. 2 *B*) predicts an apparent gating charge "Z" of 2.0 ± 0.1 ($n = 3$).

Rectification Induced by Cytoplasmic Polyamines

Membrane patches were excised into high [K^+] (K-INT) solution, with [Mg^{2+}] buffered to $<10^{-8}$ M. Under these conditions, strong rectification and time-dependent activation of inward current were initially maintained, but loss of both inward rectification and time-dependent activation of inward current always followed slowly (Lopatin et al., 1994). In most experiments, the amplitude of inward current increased initially, and this was always followed by the development of transient outward currents, until only a partial inactivation remained. Similar behavior has previously been described for inward rectification of i_{K1} channel currents in cardiac cells (Matsuda, 1988) and bovine artery endothelial cells (Silver, Shapiro, and DeCoursey, 1994). Patch current continually ran down after isolation, limiting the duration of experiments to 2–10 min, by which time the limiting time constant of inactivation at positive voltages was typically tens of milliseconds to seconds. These results are consistent with the loss of intrinsic rectification being the result of a slow dissipation of soluble components from inside the patch (Matsuda, 1988; Lopatin et al., 1994; Silver et al., 1994). Mg^{2+} ions applied to the inner surface of the membrane did cause a rapid and reversible block of HRK1 channels at positive membrane potentials. The apparent dissociation constant for Mg^{2+} was ($K_{m,+50}$) = 9.2 μM, with Hill coefficient (H) = 0.38[1] (Lopatin et al., 1994). After loss of rectification in inside-out patches, strong rectification could be restored by moving the patch back toward the oocyte surface (Lopatin et al., 1994), and this could be shown to result from release of cytoplasmic intrinsic rectifying factors (IRFs) other than Mg^{2+} from the oocyte or from other cell types (Lopatin et al., 1994). Biochemical characterization of IRFs suggested that these factors correspond to the naturally occurring polyamines (Lopatin et al., 1994).

The kinetics of block and unblock differ between each polyamine species. Relief of putrescine block (activation) is nearly instantaneous at negative voltages (Fig. 3 *A*), but the voltage-dependent unblock of spermidine and spermine is clearly resolvable. In each case, the unblock is well fitted with a single exponential without an instantaneous component (Fig. 3 *B*). Unblock activation τ increased e-fold every 15.0 ± 0.7 mV (n = 5) and 33.3 ± 6.4 mV (n = 3) for spermine and spermidine, respectively. Fig. 3 *C* shows the voltage dependence of unblock τ for spermine and spermidine (solid lines), and superimposed, the voltage-dependence of the time constants for activation of cell-attached currents (dashed lines). There is close approximation between τ_S and the time constant for recovery from spermine block, and between τ_F and the time constant of recovery from spermidine block (τ_S and τ_F taken from Fig. 1 *D*). Polyamine-induced rectification was also reversible, with the

1. Although the K_m is similar to values reported for single channel block of native strong Kir (Matsuda, 1988) and cloned IRK1 channels (Taglialatela et al., 1994), the Hill coefficient (0.38) is less than that measured for single channel current effects (~1), possibly because of additional kinetic effects of Mg^{2+}, which are not considered in single channel analysis. Because it does not correspond to a simple one-to-one binding model, it is not strictly correct to use this model for estimation of the depth (electrical distance δ) of the Mg^{2+} binding site in the voltage field.

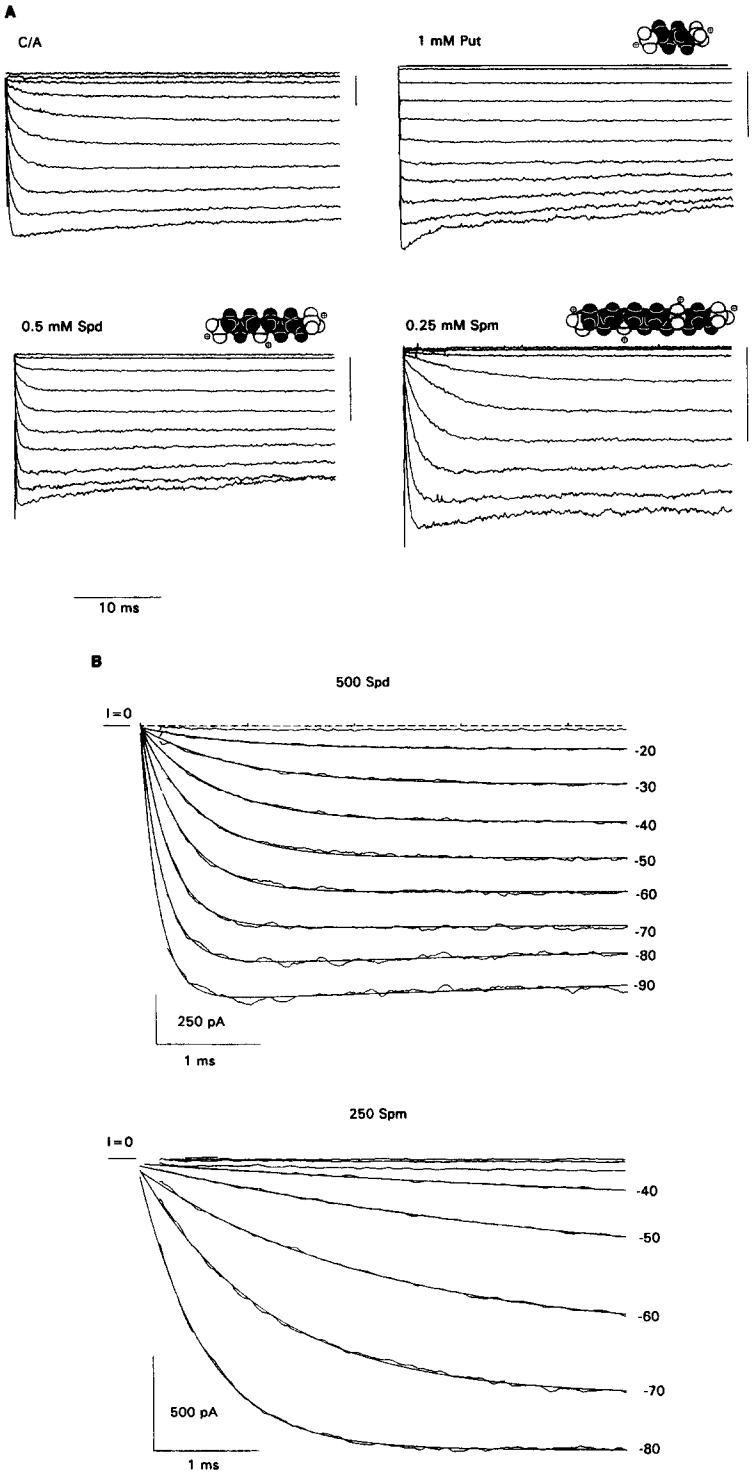
A
C/A
1 mM Put
0.5 mM Spd
0.25 mM Spm
10 ms
B
500 Spd
I=0
-20
-30
-40
-50
-60
-70
-80
-90
250 pA
1 ms
250 Spm
I=0
-40
-50
-60
-70
-80
500 pA
1 ms

FIGURE 3.

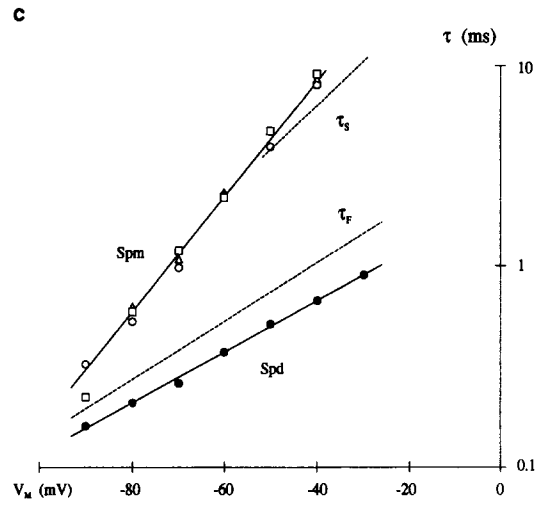

FIGURE 3. (*A*) HRK1 currents after voltage steps from +50 mV (C/A) or 0 mV to voltages between 0 and −90 mV, in cell attached (C/A) and inside-out membrane patches in the presence of 1 mM putrescine (Put), 0.5 mM spermidine (Spd), or 0.25 mM spermine (Spm). The calibration bar beside each record corresponds to 150 pA (C/A) or 100 pA. Records were corrected for capacity transients. The structure of each polyamine is indicated. Amine groups are white; methyl groups are black. (*B*) Fast time-base records of HRK1 current in response to voltage steps from +50 mV to the voltages indicated, in inside-out membrane patches exposed to 500 μM spermidine (Spd), or 250 μM spermine (Spm). Currents were corrected for leak and capacity currents and fitted with single exponentials. Currents are not shown for the first 200 μs after the voltage pulse. (*C*) Voltage dependence of the time constants for exponential fits to current activation phase in 500 μM spermidine (Spd; average data from three experiments), or 250 μM spermine (Spm, data from three individual patches are shown). Each curve is fitted with a single exponential. Also plotted (dashed) are τ_F and τ_S for the activation phase of HRK1 currents in cell-attached membrane patches (from Fig. 1 *D*).

time course of recovery being comparable with the time course of loss of rectification after patch excision (not shown).

HRK1 is one of several recently cloned strong inward rectifier K^+ channels and is expressed in heart and brain (Makhina et al., 1994; Perier et al., 1994). The first cloned inward rectifier, IRK1 (Kubo, Baldwin, Jan, and Jan, 1993), with similar expression patterns to HRK1, is only ~70% identical in amino acid sequence. However, IRK1 shows similar rectification properties in intact cells (Kubo et al., 1993). In inside-out membrane patches, inward rectification of IRK1 channels is also lost and can be restored by application of IRFs (Lopatin et al., 1994) or polyamines (Ficker, Taglialatela, Wible, Henley, and Brown, 1994). The essential properties of putrescine and spermidine block of IRK1 are the same as those of HRK1 (Fig. 4). This suggests that polyamine-induced rectification is not unique to HRK1 but is probably a major contributory factor to intrinsic rectification in all classic strong inward rectifier K channels.

Polyamine Block Shows Both Instantaneous and Time-dependent Components

Fig. 5 *A* shows currents in response to depolarizing steps from an activating voltage of −80 mV in the presence of different polyamines. There are two distinct components (instantaneous and time dependent) to block by spermine and spermidine,

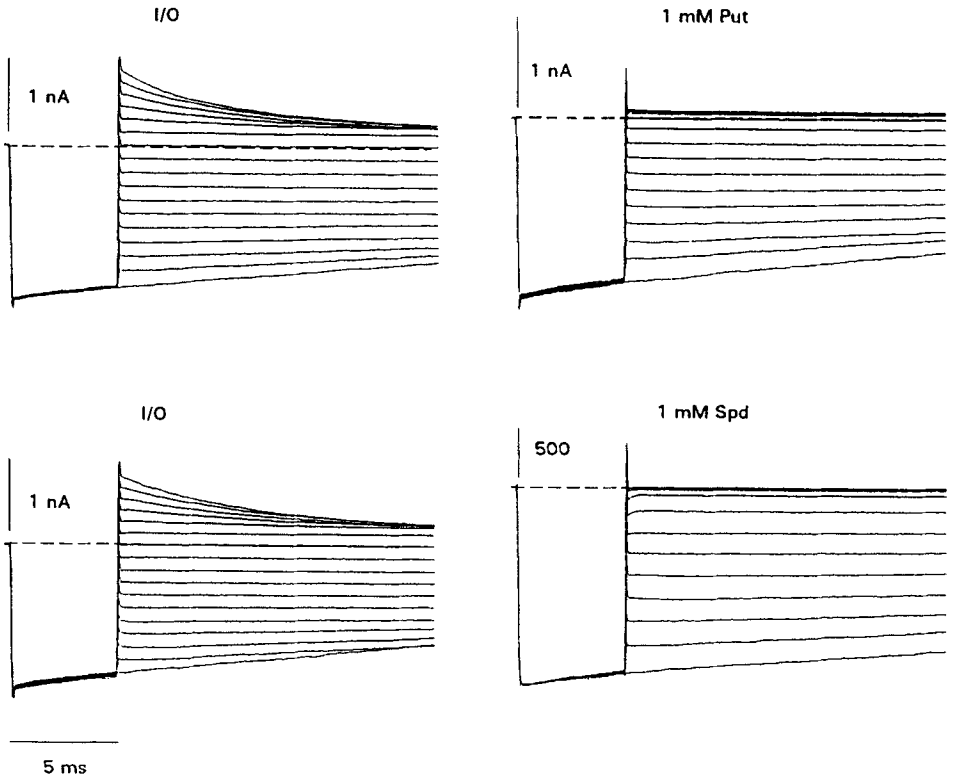

FIGURE 4. IRK1 currents after voltage steps from 0 mV to −80 mV and then to voltages between −80 and +60 mV in inside-out membrane patches in the absence of added polyamines (I/O) and after exposure to 1 mM putrescine (Put) or 1 mM spermidine (Spd). Records are not corrected for leak or capacity currents.

whereas putrescine block is nearly instantaneous. Fig. 5 *B* shows the instantaneous (dashed lines) and steady state (solid lines) relative I-Vs for 250 μM putrescine, spermine, and spermidine. Although each polyamine causes steeply voltage-dependent steady state I-V relationships, simple one-to-one channel blocking models would predict no instantaneous phase. That this is not the case is most clearly demonstrated by spermine block, for which there are fully separable instantaneous and time-dependent components to the induced rectification (Fig. 5 *B*). This behavior means that the estimated voltage sensitivity of channel rectification is critically dependent on how the I-V is measured. The instantaneous I-Vs are adequately described by single Boltzmann equations, with $Z = 1.39 \pm 0.05$ ($n = 5$), 1.61 ± 0.15 ($n = 5$), and 1.69 ± 0.15 ($n = 4$), for spermine, spermidine, and putrescine, respectively. An additional component is necessary to describe the steady state I-Vs for spermine and spermidine. Estimation of the steepness will be model dependent, but for example empirical estimation with a modified Boltzmann equation (corresponding to model IIb) gives effective valency of 5.46 ± 0.2 ($n = 5$), for sper-

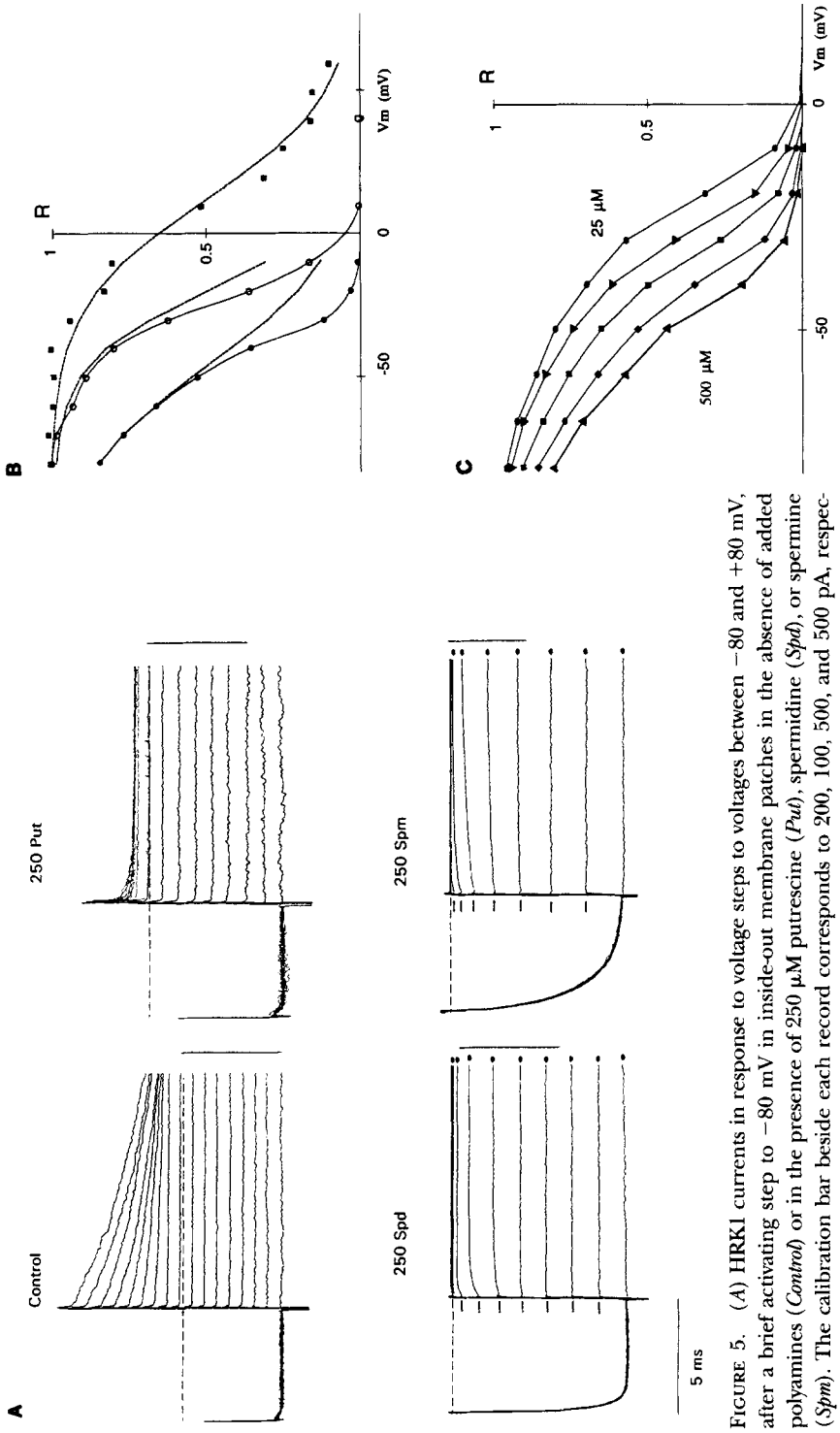

FIGURE 5. (*A*) HRK1 currents in response to voltage steps to voltages between −80 and +80 mV, after a brief activating step to −80 mV in inside-out membrane patches in the absence of added polyamines (*Control*) or in the presence of 250 µM putrescine (*Put*), spermidine (*Spd*), or spermine (*Spm*). The calibration bar beside each record corresponds to 200, 100, 500, and 500 pA, respectively. Dash and point (— and ●) symbols beside each record indicate the instantaneous and steady state currents, respectively. (*B*) Current (*R*, relative to current in the absence of added polyamines) plotted versus membrane potential for each set of currents in *A*. Points and solid curve show steady state (10 ms) relationship. Dashed line indicates instantaneous (immediately after capacity transient) relationship (see Results). (*C*) Steady state relative current (*R*)–voltage relationships for HRK1 channels in the presence of 25 (●), 50 (▼), 100 (■), 250 (◆), and 500 (▲) µM spermine.

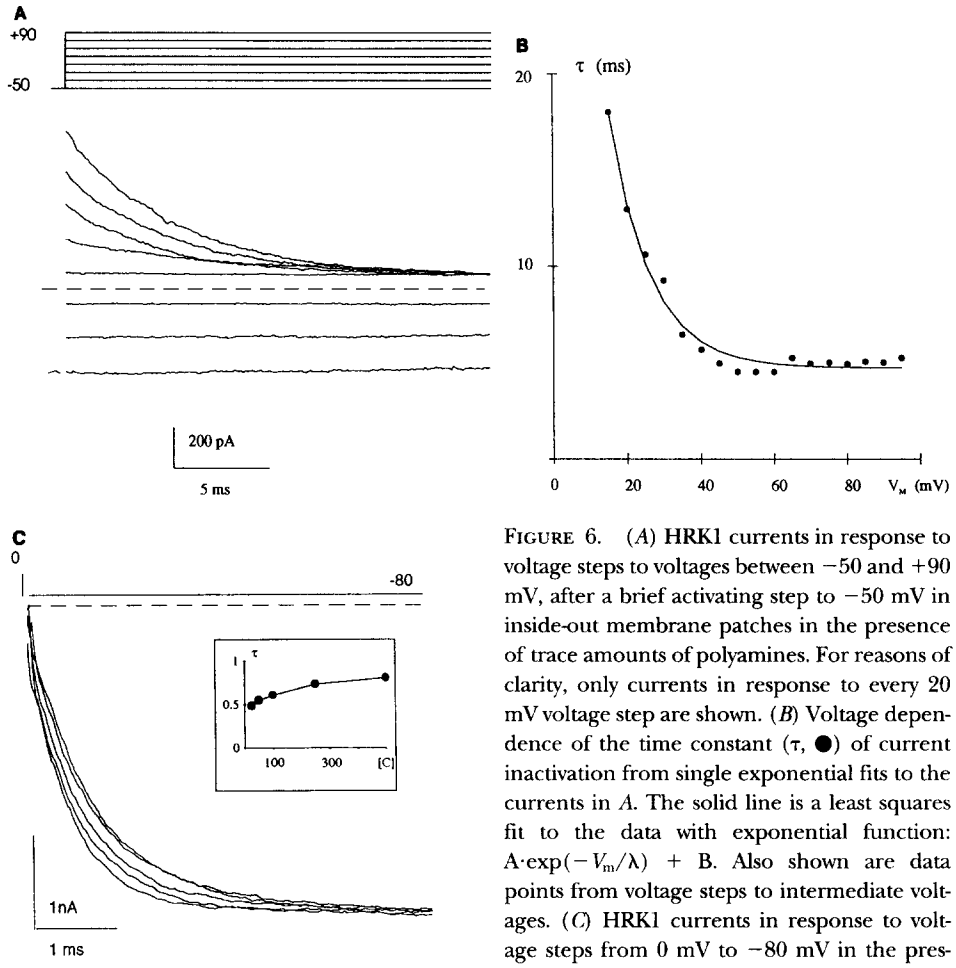

FIGURE 6. (*A*) HRK1 currents in response to voltage steps to voltages between −50 and +90 mV, after a brief activating step to −50 mV in inside-out membrane patches in the presence of trace amounts of polyamines. For reasons of clarity, only currents in response to every 20 mV voltage step are shown. (*B*) Voltage dependence of the time constant (τ, ●) of current inactivation from single exponential fits to the currents in *A*. The solid line is a least squares fit to the data with exponential function: $A \cdot \exp(-V_m/\lambda) + B$. Also shown are data points from voltage steps to intermediate voltages. (*C*) HRK1 currents in response to voltage steps from 0 mV to −80 mV in the presence of 25–500 μM spermine. Each current was fitted with a single exponential. The inset shows the concentration ([C]) dependence of the fitted time constant (τ). τ and [C] in milliseconds and μM, respectively.

FIGURE 7. General properties of polyamine block. (*A*) Voltage protocol and corresponding current traces in the presence of spermine. Filled dots and dashes show instantaneous (—) and steady state (●) components. (*B*) Current, relative to unblocked current, versus voltage for instantaneous (*Inst*, —) and steady state (*Std*, ●) components, respectively. (*C*) Both steady state (*Std*) and instantaneous (*Inst*) components of relative current shift in parallel along the voltage axis with increase of spermine concentration. (*D*) Voltage and concentration dependence of spermine block kinetics. τ of activation of inward currents (unblock, *left*) at high spermine concentration and τ of inactivation of outward currents (block, *right*) at low spermine concentrations versus membrane potential. Limiting τ of inactivation (block) changes with concentration.

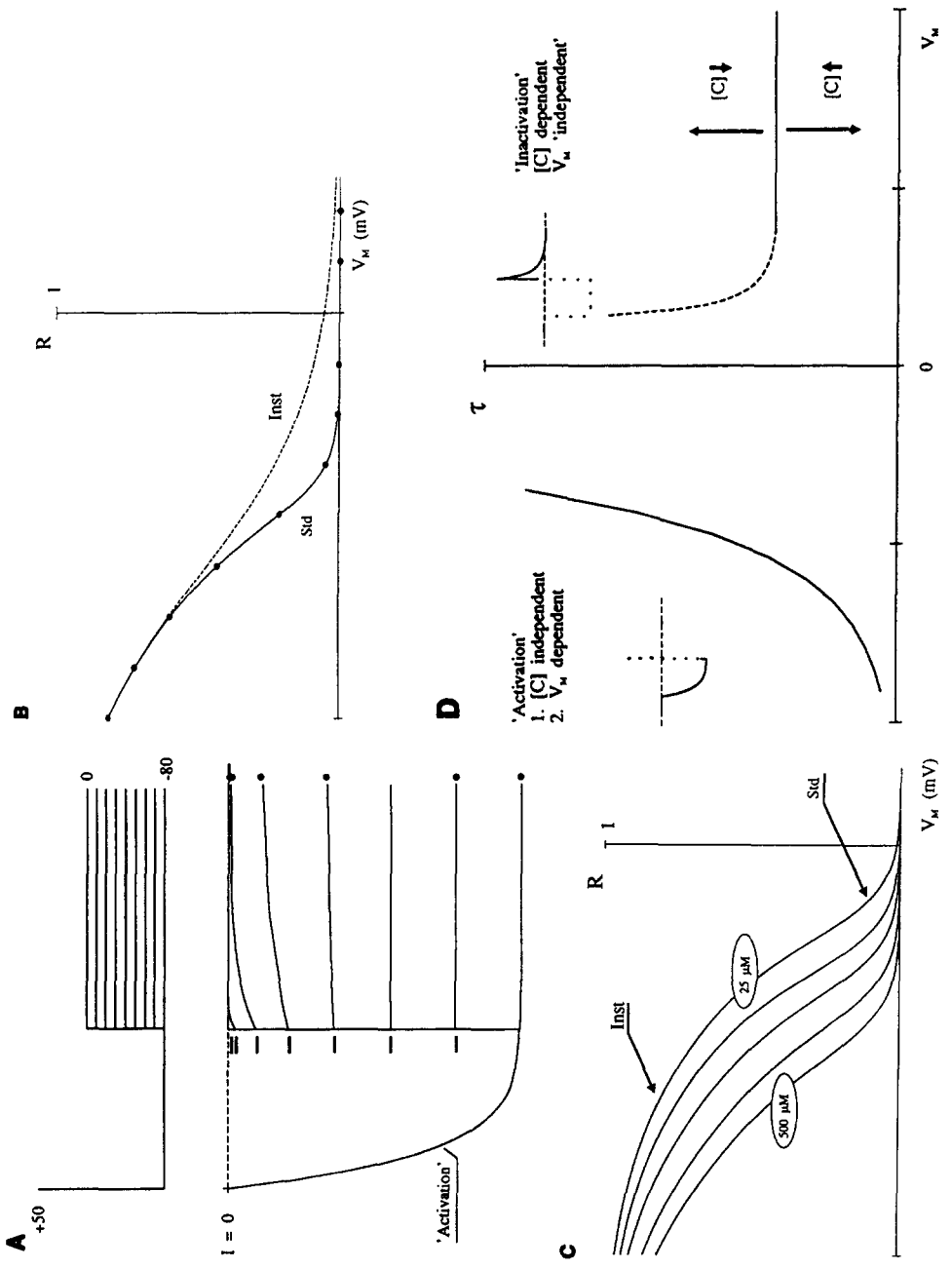
A
+50
0
-80
I = 0
'Activation'
B
R
I
Inst
Std
V_M (mV)
C
R
I
Std
Inst
25 μM
300 μM
V_M (mV)
D
'Activation'
1. [C] independent
2. V_M dependent
'Inactivation'
[C] dependent
V_M 'independent'
τ
[C]
[C]
0
V_M

FIGURE 7.

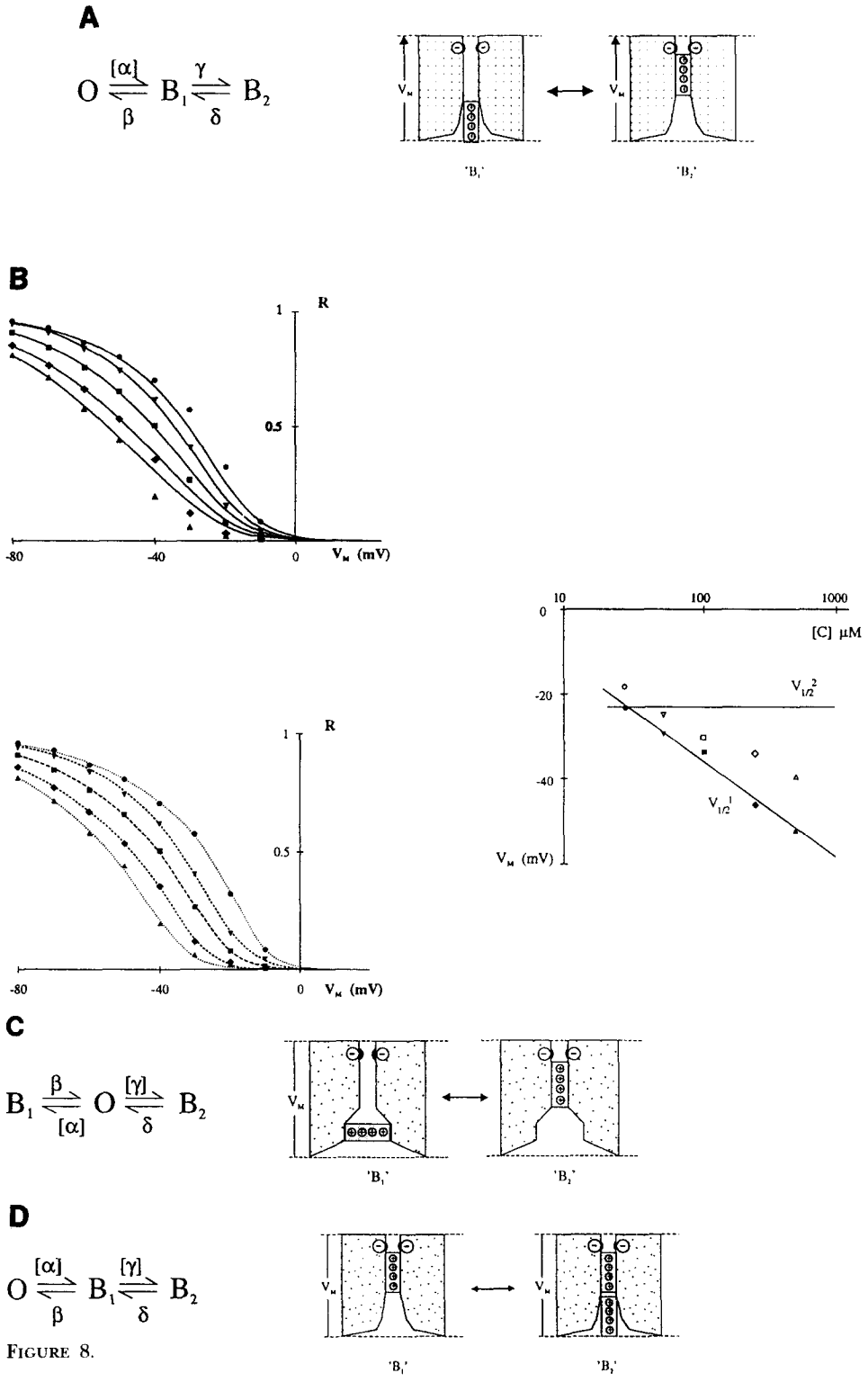
A
O ⇌ B1 ⇌ B2
[α] β γ δ
VM
'B1'
'B2'
B
R
1
0.5
-80
-40
0
VM (mV)
10
100
1000
[C] μM
-20
-40
V1/2 2
V1/2 1
VM (mV)
C
B1 ⇌ O ⇌ B2
β [α] [γ] δ
D
O ⇌ B1 ⇌ B2
[α] β [γ] δ

FIGURE 8.

mine block. As shown in Fig. 5*C*, both instantantaneous (shallow) and steady state (steep) components of spermine block are concentration dependent. We will consider these properties in detail in development of an appropriate kinetic model to explain spermine block of the channel.

Polyamine Block Kinetics Are Voltage Independent, but Unblock Kinetics Are Concentration Independent and Voltage Dependent

It was not generally possible to completely relieve inactivation of outward currents after patch excision. This may be because of an inability to completely wash out polyamines from the patch, or possibly to remove their synthesis or release from buffer systems within the patch. For this reason, examination of the kinetics of current block by quantitatively known, low concentrations of polyamines was not feasible. Fig. 6 *A* shows the voltage dependence of current inactivation in inside-out patches, presumably corresponding to block by residual traces of polyamines present within the patch. In contrast to the expectations of a simple pore-blocking model, in which a blocking particle binds at a single site within the membrane voltage field (Woodhull, 1973), the blocking rate saturates at positive voltages (Fig. 6 *B*). Because block of outward currents becomes nearly instantaneous at higher polyamine concentrations (Fig. 5 *A*), this saturating rate is clearly concentration dependent. In contrast, whereas the polyamine unblocking rate is strongly voltage dependent (Fig. 3), it is almost concentration independent (Fig. 6 *C*).

Long-pore Plugging Model for Spermine Block of Kir Channels

The simplest model for the action of a charged channel blocker (Woodhull, 1973) would predict a simple 1:1 binding of the blocking particle, which would provide monoexponential changes in current after step changes of voltage. However, it is clear from the above records (Fig. 5) that after an activation step to −80 mV, subsequent steps to depolarized potentials reveal very fast, quasi-instantaneous rectification and a slower relaxation to a steeper, stable rectification in the presence of spermine or spermidine. Conversely, after a step to a fully blocked state (+50 mV), subsequent activating steps do not reveal an instantaneous phase of recovery from block by either spermine or spermidine in the absence of other blocking poly-

---

FIGURE 8. Models with two binding sites. (*A*) Model IIa. (*Left*) One blocking molecule model kinetic scheme. [α] is concentration and voltage dependent. β, γ, and δ are voltage dependent. (*Right*) Mechanistic representation of the kinetics scheme. (*B*) (*Upper left*) Experimental (*filled symbols*) and modeled (*solid lines*) steady state I-V relationships for five different concentrations of spermine (25–500 μM). (*Lower left*) Experimental (*filled symbols*) steady state I-V relationships for five different concentrations of spermine (25–500 μM). Dashed lines are modeled fits to the individual data set at each spermine concentration. (*Right*) Dependence of $V_{1/2}^1$ (*closed*) and $V_{1/2}^2$ (*open*) on concentration, using a simultaneous fit of the model (*lines*) and individual fits at each concentration (points). (*C*) Model IIb. One blocking molecule model with two binding sites. (*Left*) Kinetic scheme. [α] and [γ] are concentration dependent. (*Right*) Mechanistic interpretation. Binding of a second moecule in state B_2 is prohibited because of electrostatic repulsion. (*D*) Model IIIa. Sequential two-blocking-molecule model. (*Left*) Kinetic scheme. [α] and [γ] are concentration dependent. (*Right*) Mechanistic interpretation. Binding of a second molecule in state B_2 is allowed.

amines or Mg^{2+} (Fig. 3 *B*). In the following, we will develop a kinetic model for polyamine binding inside the pore of HRK1 channels that can account for these observations and describe the characteristics of block by spermine and spermidine.

The data concerning spermine block were used as the standard for developing an appropriate model. Spermine is the longest of the naturally occurring polyamines (~20 Å; Fig. 3 *A*) and appears to be the most potent blocker of strong inward rectifiers (Ficker et al., 1994; Lopatin et al., 1994). Fig. 7 shows schematically the relevant voltage-dependent and concentration-dependent features of spermine block that must be accounted for by a suitable model:

1. Spermine block is strongly voltage dependent and has two distinct components: (*a*) a shallow and quasi-instantaneous (Inst) and (*b*) a slower and steeper component (Std) (Fig. 7, *A* and *B*). Because of this, steady state currents (Figs. 8 *B* and 5) are not well described by a single Boltzmann equation and require a more complex function.
2. Both the shallow (Inst) and steep (Std) part of relative currents are concentration dependent. With increasing spermine concentration, relative currents shift in parallel toward more negative membrane potentials (Fig. 7 *C*).
3. With high concentrations of spermine, activation of inward currents at negative potentials (unblock) depends strongly on voltage, but not on concentration, whereas with low concentrations of spermine, inactivation of outward currents at positive membrane potentials (block) is concentration dependent but only weakly voltage dependent (Fig. 7 *D*).

To develop a reasonable model of spermine block, the time course and concentration dependence of currents were simulated by adopting various kinetic models and kinetic parameters fitted to the experimental data. Beginning with the simplest model (model I), model complexity was increased until all experimental results could be accommodated, ensuring that the satisfactory model is a minimal one. The limitations and suitability of the models are now considered.

Model I. A simple two-state model (Eq. 1) predicts that single Boltzmann equations should describe the steady state voltage dependence of spermine block; however this is clearly not the case (Fig. 5).

$$O \underset{\beta}{\overset{[\alpha]}{\rightleftharpoons}} B \tag{1}$$

Furthermore, the on-rate of spermine block $([\alpha])^2$ should be concentration dependent, giving a decrease of the activation τ ($\tau = 1/([\alpha]+\beta)$) with an increase of spermine concentration. This is contradicted by the data, since the activation τ is essentially concentration independent or may even increase slightly with concentration (Fig. 6).

---

2. Throughout this paper, concentration-dependent rates are indicated by square brackets, such that a pure concentration-dependent rate is given by, e.g., $[\alpha] = \alpha_o * [S]$, where α_o is the first-order rate constant and [S] is the concentration of, e.g., spermine.

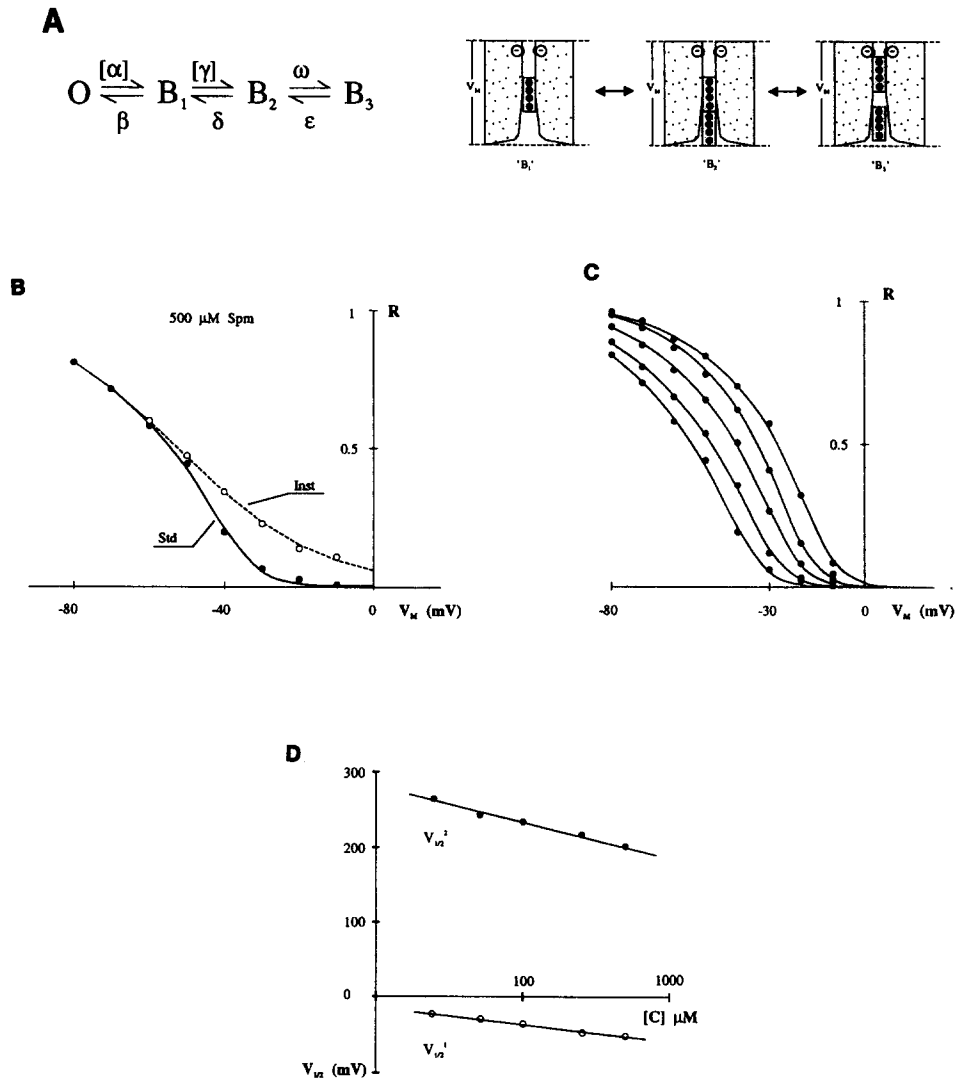

FIGURE 9. Minimal model that adequetely explains the experimental data. (*A*, *left*) Kinetic scheme. [α] and [γ] are concentration dependent; the other rate constants are only voltage dependent. (*Right*) Mechanistic interpretation. The third transition to B_3 is concentration independent and reflects further movement of the first molecule into a deep binding site. (*B*) Instantaneous (Inst, ○ experimental; dashed line, theoretical) and steady state (Std, ●, experimental; solid line, theoretical) I-V relations for 500 μM spermine. (*C*) Family of steady state I-V relationships (points, experimental; lines, theoretical) for five different concentrations of spermine (500, 250, 100, 50, and 25 μM from left to right, respectively). (*D*) Concentration dependence of $V_{1/2}^1$ (○) and $V_{1/2}^2$ (●) for $O \leftrightarrow B_1$ and $B_1 \leftrightarrow B_2$ transitions, respectively.

Models IIa and IIb. Additional complexity of the channel being blocked by one polyamine molecule at either of two sites could be obtained by having a second polyamine binding site, with one (model IIa, Fig. 8, *A* and *B*) or both (model IIb, Fig. 8 *C*) blocked sites being concentration dependent. In model IIa, the long pore of the inward rectifier channel would be considered to be blocked, or plugged, by spermine binding at the entrance of the channel pore. The spermine molecule could then undergo a further voltage-dependent transition to move deeply into the channel pore. The first blocked state (B_1) corresponds to a low affinity binding site located relatively close to the outer part of the channel pore and provides a near instantaneous block upon depolarization, with shallow voltage dependence, whereas the second binding site (B_2) is high affinity and located deeply in the pore, providing the steep part of the steady state I-V curve. The slow backward transition to state B_1 would provide a slow, concentration-independent phase of activation.

As indicated in Fig. 7 *D*, the limiting rate of block at depolarized potentials is concentration dependent but voltage independent. Model IIa can accommodate this finding because of voltage independence of the first blocking reaction ($O \leftrightarrow B_1$; Fig. 8 *A*). In Fig. 8 and subsequent figures, rate constants inside rectangular brackets are concentration dependent,[2] whereas other rate constants are voltage dependent. Thus, at any [spermine], the rate constant for the first blocking reaction ($O \leftrightarrow B_1$) becomes rate limiting in determining the relaxation τ ($\tau \rightarrow 1/[\alpha]$) at positive potentials, since the off-rate (β) approaches zero (see Appendix). Simultaneous fitting of model IIa to the full data set gives $Z_2 = 2.8$ and a concentration-independent $V_{1/2}^2 = -23.6$ mV (Fig. 8 *B*). However, it is apparent from Fig. 8 *B* that this model cannot reproduce the concentration-dependent shift of the steep components of the steady state I-V curve. Independent fitting of the model to steady state (and instantaneous, not shown) I-V curves at each concentration of spermine (Fig. 8 *B, below*) provided excellent fits, demonstrating that both blocking transitions should be concentration dependent, the concentration dependence of $V_{1/2}^2$ (the equilibrium voltage for transition $B_1 \leftrightarrow B_2$), is as steep as the concentration dependence of $V_{1/2}^1$ (the equilibrium voltage for transition $O \leftrightarrow B_1$). For individual fits (Fig. 8 *B, below*), calculated "effective valencies" Z_1 and Z_2 are 1.45 ± 0.06 ($n = 5$) and 3.9 ± 0.3 ($n = 5$), respectively. Z_1 is reasonable, but $Z_2 = 3.9$ would require that all four charges of the spermine molecule pass nearly 100% of the membrane electric field during the transition. This seems unrealistic and does not leave "space" for the $O \leftrightarrow B_1$ transition.

A similar but nonsequential model (model IIb) that allows only one molecule to be inside the channel pore was also considered (Fig. 8 *C*). In this model, because of the linear structure of spermine, two conformations of block might be suggested: in site B_1, spermine cannot undergo deep transition because of steric limitations, whereas in state B_2, the spermine molecule will lie within the narrow pore. Only one molecule could reside within the channel at any given time. Each transition ($O \leftrightarrow B_1$ and $O \leftrightarrow B_2$) is concentration dependent, accounting for concentration dependence of $V_{1/2}^1$ and $V_{1/2}^2$. Again, this model gave excellent fits to steady state and instantaneous I-V curves at each [spermine] (not shown). However, this model required an even higher effective valency Z for transition $O \rightarrow B_2$ than the previous

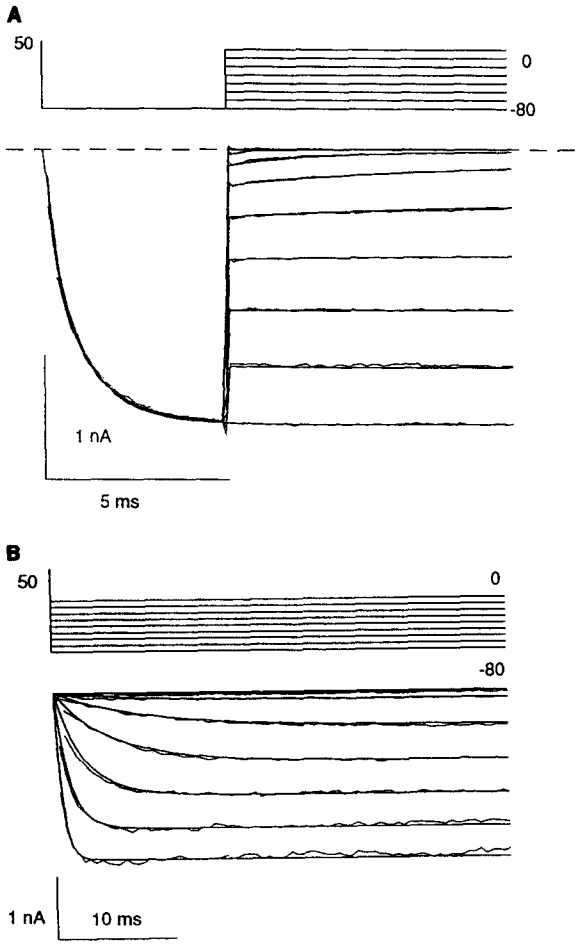

FIGURE 10. Kinetics of HRK1 inward currents in the presence of 250 μM spermine. (*A*) Currents are shown in response to voltage steps from +50 mV to −80 mV and then to voltages between −80 mV and 0 mV, in 10 mV increments. Theoretical currents (*smooth lines*) are superimposed on real currents. (*B*) Currents in response to voltage steps from +50 mV to voltages between −80 mV and 0 mV. Theoretical currents (*smooth lines*) are superimposed on real currents. Experimental current traces were leak and capacity subtracted before manual fitting (see Methods).

model: $Z_1 = 1.40 \pm 0.02$ ($n = 5$) and $Z_2 = 5.46 \pm 0.2$ ($n = 5$), and for this reason was also unrealistic.

The above results argue that appropriate explanation of the data requires consideration of more complex kinetics schemes with more than one spermine molecule involved in blocking or more than two blocked configurations. We next considered the possibility that the pore of the channel may be physically long enough to accept at least two spermine molecules. We show below that, on theoretical grounds, we may reject the limitation of only one molecule inside the pore (because of electrostatic repulsion), and that permitting multiple ions to reside within the pore may provide the correct kinetic scheme.

Models IIIa and IIIb. The sequential kinetic scheme (model IIa) from the previous section (Fig. 8 *A*) was taken as a basis for further modeling. As shown above, this model cannot account for concentration dependence of the second transition ($B_1 \leftrightarrow B_2$) and suggests that a second molecule is involved in the blocking process. A possible physical basis for such a model (model IIIa) is shown in Fig. 8 *D*. Al-

though this differs from the model involving one blocking molecule, it is formally related and suffers from the same intrinsic problems: a high value of effective valency Z_2 (3.9), which should be less than Z_1 (1.45), since the second molecule should not enter as deeply as the first. To provide near-instantaneous rectification after a depolarizing voltage step (Figs. 5 and 7), [α] and β must be high. Furthermore, the concentration-dependent approach rate to the second binding site should be as fast as the rate of approach to the first site, such that [γ] must also be as high as [α]. Since $V_{1/2}{}^2$ for the second transition ($O \leftrightarrow B_2$) is in the range of −20 to −50 mV, then in this voltage range, the "off" rate (δ) should also be as high as [γ] (and [α] and β), which in turn leads to extremely fast (instantaneous) transitions from both blocked states B_1 and B_2 to the open state O, contradicting the experimentally observed slow activation of inward currents (Fig. 7 *A*).

However, a small modification to this model, formally introducing a third, concentration-independent block state (model IIIb) is able to explain all the experimental data, including the steady state I-V and kinetic measurements (Fig. 9). Such a model could be accommodated in the following physical arrangement. We postulate that (*a*) the channel pore is long enough to contain two molecules of spermine

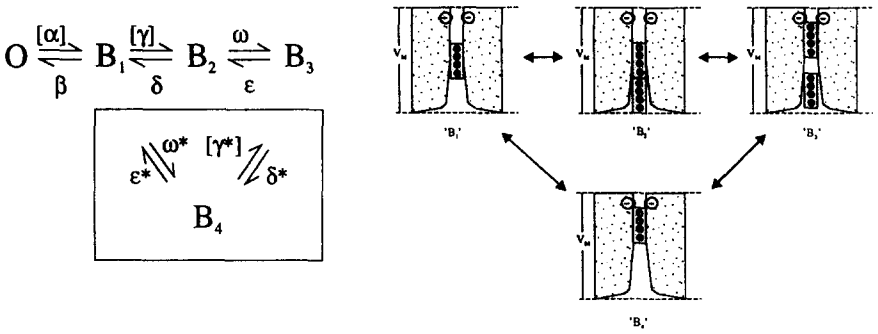

FIGURE 11. Complete mechanistic model for polyamine-induced inward rectification. (*Left*) Kinetic scheme. [α] and [γ] are concentration dependent. (*B*) Mechanistic interpretation.

at a time and that they enter the pore sequentially; (*b*) the binding of spermine at each site is voltage independent; (*c*) there is an electrostatic repulsion between two spermine molecules inside the pore; and (*d*) there is at least one voltage-dependent transition deep in the pore.

With more variables than in the $O \leftrightarrow B_1 \leftrightarrow B_2$ model, it is easier to fit the same set of experimental data. "Blind" fitting of the $O \leftrightarrow B_1 \leftrightarrow B_2 \leftrightarrow B_3$ model to the instantaneous and steady state I-V curves gives several solutions (because of multiple local minima of a control sum with a least square algorithm). However, most do not match kinetics or are unrealistic for other reasons. Only the following solution (major minima of a control sum) meets all requirements of the experimental data and has a plausible mechanistic explanation (Fig. 9). Simultaneous fitting of all steady state data gave the following values for effective valencies Z_i : Z_1 = 1.39, Z_2 = 1.34, and Z_3 = 2.68 for each transition, respectively. With these values for Z_i, the

problem of extra charge movement (>4) during a given transition disappears. The concentration-independent $V_{1/2}{}^3 = -160$ mV (see Appendix) and the concentration dependence of $V_{1/2}{}^1$ and $V_{1/2}{}^2$ are presented in Fig. 9. We would interpret the extremely positive values for $V_{1/2}{}^2$ and very negative values for $V_{1/2}{}^3$ as a reflection of the electrostatic repulsion felt between the two spermine molecules at state B_2. Kinetic data were then fitted by varying individual rate constants. Concentration and voltage-independent rate constants were $\alpha_o = 37.6\ s^{-1}\mu M^{-1}$, $\beta_o = 860\ s^{-1}$, $\gamma_o = 37.6\ s^{-1}\mu M^{-1}$, $\delta_o = 7.8 \cdot 10^8\ s^{-1}$, $\epsilon_o = 13.0\ s^{-1}$, $\omega_o = 1.9 \cdot 10^8\ s^{-1}$. All time-dependent characteristics of ionic currents are well reproduced. Fig. 10 shows theoretical currents generated by the use of the model (noiseless lines) superimposed on real data for two different voltage protocols. The same set of parameters was used with different concentrations of spermine and at all different membrane potentials. This model also reproduced voltage independence of inactivation of outward currents at positive membrane potentials with a low concentration of spermine (not shown).

Modeling of Block by Other Polyamines

The same kinetic scheme was then used to model the kinetic and steady state block of Kir channels by spermidine. We have shown (Lopatin et al., 1994) that the actions of spermine and spermidine are qualitatively similar. However, the block by spermidine is ~10-fold less effective than the block by spermine, and the kinetics of block and unblock are faster. For this reason, the data set for spermidine is noisier and less reliable than that for spermine and was not used for primary determination of the general model. However, having obtained the appropriate model to describe spermine action (above), we adopted the strategy of taking the spermine model with fitted parameters, then scaling the effective valency of voltage-dependent transitions by 3/4(for spermidine^{3+} versus spermine^{4+}). We fit the first instantaneous rectification ($O \leftrightarrow B_1$ transition) by changing the "off" rate $\beta(V)$, and then fit the rest of the model. As for spermine, all kinetic and steady state data for spermidine were well fit with the single set of rate constants for all voltages and concentrations tested. The major quantitative difference between the two models is that (a) effective valency (Z_1) for the $O \leftrightarrow B_1$ transition was slightly higher, 1.61 ± 0.14 ($n = 5$), than for spermine.

We have not modeled putrescine block in detail, because the kinetics are too fast to be resolved by our recording system. However, the above model could accommodate all available steady state data with appropriate scaling of the effective valency of voltage-dependent transitions by 2/4 (for putrescine^{2+} versus spermine^{4+}).

DISCUSSION

"Intrinsic" Rectification of Kir Potassium Channels

Since the original descriptions of inward rectification of potassium conductance (Katz, 1949; Noble, 1965), it has been realized that rectification is a time-dependent process and that activation of the current at negative voltages can follow a multiexponential time course (Hagiwara et al., 1976; Stanfield et al., 1981; Kurachi,

1985; Ishihara et al., 1989; Oliva et al., 1990). As first reported by Vandenberg (1987) and Matsuda et al. (1987), cytoplasmic Mg^{2+} ions cause voltage-dependent block of Kir channels (Lopatin et al., 1994; Armstrong, 1969; Hille and Schwartz, 1978) and are likely to be responsible for at least part of the nearly instantaneous activation of HRK1 after a hyperpolarizing voltage step (Fig. 1 *C*). However, previous studies have reported that, even in the absence of Mg^{2+}, a time-dependent, strong rectification of the Kir current still occurs, and the steady state I-V is essentially not different in the absence or presence of Mg^{2+} (Saigusa and Matsuda, 1988; Ishihara et al., 1989; Burton and Hutter, 1990; Silver and DeCoursey, 1990; Ishihara and Hiraoka, 1994; Stanfield, Davies, Shelton, Khan, Brammar, Standen, and Conley, 1994a). Subsequent investigations have relied on empirical models to explain the non–Mg^{2+}-dependent component of rectification (Cohen, DiFrancesco, Mulrine, and Pennefather, 1989; Ishihara et al., 1989; Pennefather, Oliva, and Mulrine, 1992; Pennefather and De Coursey, 1994) and have tended to implicitly consider that strong rectification involves an intrinsic gating or conformational change of the channel protein. The channel is said to activate with hyperpolarization and inactivate or deactivate at positive potentials, the voltage sensitivity of the gate being allosterically modulated by external K^+ ions. We have confirmed the original observation of Matsuda (1988) that intrinsic rectification disappears with time after excision of a membrane patch from the cell (Lopatin et al., 1994). The demonstration that this loss of rectification can be reversed simply by moving the patch close to the depolarized cell membrane (Lopatin et al., 1994) suggests that the underlying mechanism is not an irreversible process such as phosphorylation or destruction of a necessary cellular structure. Partial purification of active factors allowed us to determine essential biochemical features that together strongly suggest that cytoplasmic polyamines are responsible for intrinsic rectification (Lopatin et al., 1994).

As shown in Fig. 1, intrinsic gating in intact cells follows a complex multiexponential time course. The present results can explain this finding by assuming that during depolarizations, one of multiple species of polyamines or Mg^{2+} will be occupying, and blocking, any given channel. After a hyperpolarizing step, the fraction blocked by each species will open with a characteristic time course. As shown in Fig. 3, the time constants for current activation in cell-attached patches closely match the measured time constants for spermine, spermidine, and putrescine (instantaneous) unblock. Spermine, spermidine, and putrescine are all estimated to be present in *Xenopus* oocytes at free concentrations of 300–700 μM (Osborne, Mulner-Lorillon, Marot, and Belle, 1989); hence all should be significant contributors to inward rectification in vivo. Such concentrations would predict that even inward currents should be substantially inhibited by spermine and spermidine over the full voltage range examined in the present experiments. That this is indeed the case seems to be the explanation for the increase in *inward* currents at voltages as negative as −80 mV as a consequence of patch excision (Lopatin et al., 1994).

Implications of Polyamine Action for Cellular Physiology

The present results may help to explain the wide variety of inwardly rectifying channel properties observed in nature, and in particular in the nervous system, where

there appears to be a spectrum of kinetic properties of inwardly rectifying channels. Although some channels show almost instantaneous and steep rectification, others have very slow kinetics or shallow rectification (Kandel and Tauc, 1966; Constanti and Galvan, 1983; Hestrin, 1987; Inoue, Nakajima, and Nakajima, 1988; Williams, Colmers, and Pan, 1988; Brismar and Collins, 1989; Newman, 1993). This could arise from channels with similar properties being located in cells with differing relative concentrations of polyamines (Shaw, 1994) or from channels having differing relative or absolute sensitivities to polyamine binding.

Polyamines are present in almost all known cells (Tabor and Tabor, 1984). Putrescine and cadaverine can be synthesized by decarboxylation of ornithine and lysine, respectively. Spermidine and spermine are synthesized from putrescine and decarboxylated S-adenosylmethionine (Bachrach, 1973). Spermine and spermidine are reported to be essential for normal and neoplastic cell growth (Pegg and McCann, 1980) and may have a role as stabilizing moieties for DNA; however, other molecular actions of these compounds are not clear. Some of the diverse biological effects of these compounds could be related to their induction of intrinsic rectification in potassium channels. As a general concept, increasing levels of polyamines will increase the degree of rectification and increase excitability. Many tumors contain high levels of polyamines, and polyamine analogues may be useful anticancer therapies (Feuerstein, Szollozi, Basu, and Marton, 1992; Basu, Pellarin, Feuerstein, Shirahata, Samejima, Deen, and Marton, 1993). Epilepsy and cardiac hypertrophy are each associated with both enhanced cellular excitability and elevated polyamine levels (Caldarera, Orlandini, Casti, and Moruzzi, 1974; Bartolome, Huguenard, and Slotkin, 1980; Laschet, Trottier, Grisar, and Leviel, 1992b; Hayashi, Hattori, Moriwaki, Lu, and Hori, 1993; Mialon, Cann-Moisan, Barthelemy, Caroff, Joanny, and Steinberg, 1993). Conceivably, cell proliferation and seizure activity could involve what may only need to be subtle changes in rectification at negative membrane potentials. Polyamine levels inside cells can be altered pharmacologically using analogue inhibitors of ornithine decarboxylase (Tabor and Tabor, 1984), and this could be the basis for a therapeutic modulation of inward rectifier currents. Polyamines have been found to have complex interactions with NMDA receptor channels (Williams, Romano, Dichter, and Molinoff, 1991; Scott, Sutton, and Dolphin, 1993), and although extracellular polyamine levels are normally low, it has been suggested that spermine and spermidine may enhance excitability in the brain via actions at the NMDA receptor (Scott et al., 1993). Our results suggest an alternative possibility in that changes of *cytoplasmic* polyamine levels will alter the degree of rectification of inward rectifier channels, and hence increased cytoplasmic polyamine levels could be excitotoxic. Given the steep voltage dependence of polyamine action, it is likely that the cytoplasmic concentration will always be within the dynamic range of effect at some voltage, such that even small changes of polyamine levels could have significant effects on excitability.

The Mechanism of Polyamine-induced Inward Rectification

Many nonbiological compounds containing charged primary, secondary, or tertiary amines are found to block potassium channels (Hille, 1992), and as far back as 1969, Armstrong noted the resemblance between voltage-dependent block by

TEA^+ and inward rectification. In 1978, Hille and Schwartz made a detailed mathematical analysis of the physical constraints required for rectification to result from block of the channel by a positively charged particle. Probably the greatest obstacle to invoking a channel pore blocking mechanism for inward rectification has been to explain the steepness of the voltage dependence (Z = 2–5), since Mg^{2+} block is not steep enough (Z = 1.12; Lopatin et al., 1994). Silver, Shapiro, and DeCoursey (1994) specifically considered the possibility that a blocking particle could be responsible for Kir intrinsic gating and rejected the hypothesis on the grounds that the voltage dependence was too steep for a monovalent or divalent blocking particle. Many studies have demonstrated that Mg^{2+} ions often share binding sites on proteins with polyamines (Seiler, 1994). Although polyamine actions on NMDA receptors are complex (Romano and Williams, 1994), it now seems that part of the effect could be explained by external inorganic cations and polyamines binding at similar sites in the external mouth of the receptor (Reynolds, 1992) and blocking the channel pore. The characteristics of polyamine-induced rectification above lead us to propose that these polycationic compounds cause inward rectification by a classic channel-pore–blocking mechanism, binding in the Kir channel at the same binding site as Mg^{2+}. Internally applied polyamines have only weak blocking effects on K^+ channels and Ca^{2+} channels that do *not* show high sensitivity to Mg^{2+} block (Scott et al., 1993; Ficker et al., 1994; Lopatin et al., 1994). In IRK1 channels, both high Mg^{2+} affinity and intrinsic rectification depend on the presence of a negatively charged residue in transmembrane domain M2 (Lu and MacKinnon, 1994; Stanfield, Davies, Shelton, Sutcliffe, Khan, Brammar, and Conley, 1994b; Wible, Taglialatela, Ficker, and Brown, 1994). Introducing a negative charge at this site (N171D) into the normally weak, inwardly rectifying ROMK1 converts the channel into a strong inward rectifier (Lu and MacKinnon, 1994) and induces a high sensitivity to block by internal spermine (Lopatin et al., 1994). Because of the high charge on polyamines, a steep voltage dependence is predicted for a pore blocking mechanism (see below). We cannot exclude the possibility that the polyamine action on Kir channels involves an allosteric action outside the channel pore, but the parallels between polyamine action and Mg^{2+} action argue that this is unlikely to be the case.[3]

Complex Kinetics of Polyamine-induced Rectification

The complex kinetics of polyamine block cannot be explained by a simple two-state model. One of the important findings to be accounted for in the modeling of polyamine action is the phenomenon of instantaneous rectification (Fig. 7), followed by slow relaxation to steady state. Both instantaneous rectification (or fast block) and slow activation of inward currents (or slow unblock) can be observed in

3. We have considered the possibility that an electrostatic tuning mechanism could be responsible, whereby polyamines binding to the inner surface of the channel, without voltage-dependent binding, could cause rectification by lowering the effective $[K^+]$ at the inner mouth (Lu and MacKinnon, 1994). However, no matter how high the surface charge density (Φ) is raised, it is impossible to obtain the steepness of rectification around E_K that is observed experimentally.

the same (negative) range of membrane potentials, requiring more than one binding site. We were initially suspicious about the purity of the polyamines examined. Although we used fresh solutions, it is possible that the commercially supplied spermine and spermidine (Sigma Chemical Co., St. Louis, MO) were contaminated with inorganic cations or with degradation species having fast channel-blocking kinetics, which could potentially explain the presence of both instantaneous rectification and slow activation. We cannot exclude the possibility of contamination by inorganic cations, but they seem to be an unlikely explanation, since amino acids and other related compounds from the same commercial source do not induce any instantaneous rectification. The possibility of degradation of longer polyamines to smaller ones (or contamination with them) was rejected after mass spectrometry analysis.[4]

In contrast to the voltage-dependent block by Mg^{2+} ($Z = 1.12$–1.18; Lopatin et al., 1994; Wible et al., 1994), the steepness of polyamine-induced rectification is high enough to explain strong rectification seen in intact cells. However, the question of the steepness of in vivo rectification is not trivial. Since at least two phases of rectification are present, fast and slow (Fig. 1), estimation of steady state rectification depends on how it is made. We initially estimated steady state by measuring currents at the end of the test voltage pulse (Lopatin et al., 1994). This caused underestimation of the steepness because of the slow phase of polyamine block (Fig. 5), especially at membrane potentials close to 0 mV. Unfortunately, the use of longer voltage pulses introduces additional artefacts, since it appears to speed up the rate of channel rundown and causes secondary voltage-dependent and time-dependent effects on both HRK1 current (Fig. 1) and endogenous oocyte Cl^- currents (Miledi and Parker, 1984). For these reasons, we used exponential fitting procedures to estimate both steady state and instantaneous rectification. The estimated steepness of steady state rectification in vivo, and induced by polyamines then varies with voltage, between $Z = 1.39$ and $Z = 5.46$, which matches the steepness reported for native Kir channels (Hille, 1992) and accounted for by the present modeling (Fig. 9). Complex shapes of steady state I-V relationships have been described in other preparations of native Kir channels (Leech and Stanfield, 1981).

An Adequate Model to Describe Polyamine-dependent Gating

Although a four-state sequential model (model IIIb, Fig. 9) is fully adequate to fit all experimental data, it lacks full compatibility with simple structural probabilities. Given the assumed physical implications of the model, there should be at least one additional pathway leading directly to, and out of, the deep binding site (i.e., $O \leftrightarrow B_3$). Fig. 11 shows a complete kinetic scheme compatible with the physical reality of channel block by two polyamine molecules. The additional transition $B_4 \leftrightarrow B_3$ corresponds to the block and unblock by a second molecule of spermine when a

4. Samples of spermine, spermidine, putrescine, and cadaverine were analyzed by mass spectrometry (Vestec Electrospray, Vestec Corp., Houston, TX) operating in the positive ion mode. Samples were infused at 5 ml/min in 50% CH_3CN, 3% ethanol. The spermine and spermidine spectra contained no detectable peaks corresponding to putrescine or cadaverine.

first one resides in the deep binding site. The transition $B_1 \leftrightarrow B_4$ is voltage dependent but concentration independent, whereas transition B4 $\leftrightarrow$ B3 is concentration and voltage dependent.[5]

Therefore, the sequential model $O \leftrightarrow ... \leftrightarrow B_3$ (Fig. 9), which describes the experimental data, requires additional modifications to aquire complete mechanistic integrity, and the complete scheme (Fig. 11) is more complex than is required to explain the available data set. We assigned reasonable values for the rate constants describing transitions involving the B_4 state and their voltage sensitivity ($[\gamma^*_o] = [\gamma_o]$, $\delta^*_o = 47\ s^{-1}$, $\epsilon^*_o = \epsilon_o$, $\omega^*_o = 13\ s^{-1}$, $Z_{B1\leftrightarrow B4} = 2.65$, $Z_{B4\leftrightarrow B3} = 1.37$, with thermodynamic reversibility. The values assigned to δ^*_o and ω^*_o are much lower than δ_o and ω_o, reflecting the lack of electrostatic repulsion in state B_4 compared with state B_2. Simulations using these additional rate constants showed: (1) the additional state (B_4) does not change the overall behavior from that of the sequential model (Fig. 10), and (2) this state does not affect absolute values of the rate constants in the sequential part of the model. Both steady state and kinetic data were well fit with the complete model (Fig. 11) using rate constant for $O \leftrightarrow ... \leftrightarrow B_3$ transitions obtained in Results.

Implications of the Modeling—"Long-pore Plugging" of the Kir Channels by Polyamines

Classical biophysical studies on Kir channels have suggested that the channel may consist of a long narrow pore (Hille and Schwartz, 1978; Hille, 1992). One potentially useful aspect of the current modeling is that, for the first time, it provides some reasonably concrete predictions about physical dimensions inside the Kir pore, rather than just electrical equivalent distances. The simple three-dimensional structures of natural polyamines (Fig. 3) could make them useful tools for mapping the geometrical structure of the pore region of strong inward rectifiers. The calculated length of the spermine molecule is about 20 Å. Model III requires that two molecules block the channel in a sequential manner. Assuming that the molecules enter the channel end-to-end (vertically), the proposed length of the pore region should be at least 20·2 = 40 Å. These predictions are in line with the channel really consisting of a long, narrow pore that is essentially "plugged" by the polyamines.

Several lines of argument seem to lend support to the suggestion that the polyamine molecules enter and block the channel vertically, rather than side-on (horizontally), or folded. First, experimental measurements of the size of ions capable of permeating K^+ channels (Hille 1992) predict a limiting pore diameter of about 3.3 Å, such that the spermine molecule (diameter ~4 Å) could not actually pass through the channel, even vertically. Second, both of the concentration-dependent rate constants in transitions $O \leftrightarrow B_1$ and $B_1 \leftrightarrow B_2$ ($[\alpha]$ and $[\gamma]$) are es-

5. It can be shown that the pathway $O \leftrightarrow B_1 \leftrightarrow B_4 \leftrightarrow B_3$ alone (which was not considered in Results) cannot suffice to explain the experimental data, again because it requires extremely high values for effective valency (Z) of the blocking particle during the $B_1 \leftrightarrow B_4$ transition. Furthermore, none of the rate constants would reflect the reasonable suggestion of electrostatic repulsion between two blocking molecules inside the pore.

sentially voltage independent for both spermine and spermidine block. This model prediction means that the conduction pathway is blocked immediately when the molecule enters the pore, essentially without having to enter the electrical field of the membrane. If the mouth of the pore at the beginning of the electrical field were as wide as 20 Å (to accept the spermine molecule in the horizontal orientation), then at the same depth, spermine in the vertical orientation would not be wide enough to block K^+ ion entry into the pore, and deeper penetration would be necessary to stop ion flow, which in turn would require voltage dependence of the "on" rates [α] and [γ].

There is now considerable evidence that an aspartate residue (D171) in the second transmembrane domain of IRK1 underlies high sensitivity to channel block by both Mg^{2+} and polyamines (Ficker et al., 1994; Stanfield et al., 1994*b*; Wible et al., 1994) and that introduction of an aspartate residue at the equivalent site in ROMK1 (N171D mutation) introduces high sensitivity to block by Mg^{2+} ions and polyamines (Lopatin et al., 1994; Lu and MacKinnon, 1994). It is tempting to speculate that one or both of the deep binding states in the model (B_2, B_3) correspond to polyamine binding at, or near to, this site.

Comparison with Previous Models of Inward Rectification and Mg^{2+} Block

Previous models of intrinsic rectification, using a much more limited data set from intact cells or membrane patches that probably still contain substantial but unknown concentrations of polyamines, have generally been able to adequately explain the data assuming a three-state model:

$$C \rightleftharpoons O \rightleftharpoons B \qquad (2)$$

where C is a closed state that is equivalent to the lumped polyamine blocked states in the current modeling, O is the open state, and B is the Mg^{2+} blocked state (Leech and Stanfield, 1981; Ishihara et al., 1989; Oliva et al., 1990; Stanfield et al., 1994*a*). If the $O \leftrightarrow B$ transition is instantaneous, or is absented by removal of Mg^{2+}, then such a model predicts single exponential current decays after a voltage step and might reasonably well describe the results for a fixed concentration of polyamine(s). However, as discussed above, such a model cannot explain the complex kinetics observed at different [polyamine]. Two related observations involving the interactions of Mg^{2+} ions with the Kir channel and with intrinsic gating have been considered mechanistically in detail (Matsuda, 1988; Ishihara et al., 1989; Oliva et al., 1990; Stanfield et al., 1994*a*) and require consideration here. First, internal Mg^{2+} ions have been shown to slow the closure of the intrinsic gate (Ishihara et al., 1989; Stanfield et al., 1994*a*). This is easily explained by assuming that Mg^{2+} ions gain competitive access to some or all of the polyamine binding sites in the channel pore (Lopatin et al., 1994; Lu and MacKinnon, 1994; Stanfield et al., 1994*a*; Wible et al., 1994;). Second, at intermediate blocking concentrations, internal Mg^{2+} and external Cs^+ or Ba^{2+} have been reported to block the Kir channel in three discrete steps (Matsuda, 1988; Matsuda, Matsuura, and Noma, 1989), and this has been taken as evidence that the Kir channel is formed of three functionally dependent pore forming units, a triple-barreled arrangement (Matsuda et al., 1989).

Ishihara et al. (1989) and Oliva et al. (1990) incorporated this behavior in a more detailed kinetic scheme:

$$C \rightleftharpoons O \rightleftharpoons 2/3O \rightleftharpoons 1/3O \rightleftharpoons B, \quad (3)$$

where C is the closed state, O is the fully open state, and 2/3O and 1/3O are partial conducting states in which one or two of the three barrels are blocked by Mg^{2+}. This model predicts that intermediate concentrations of Mg^{2+} will actually enhance Kir current at voltages where the channel is largely intrinsically closed (blocked by polyamines), i.e., at potentials positive to E_K. Because of technical problems with examining the effects of Mg^{2+} on HRK1 channels (Mg^{2+} speeds up the rate of channel rundown), we have not been able to examine the possibility that Mg^{2+} can enhance the current that is partially blocked by exogenous polyamines. We have no evidence to contradict the possibility that the Kir channel is triple barreled. The present model would work equally well for *independent* polyamine block of each barrel of a triple-barreled channel. However, previous studies of intrinsic channel closure (polyamine block) in the absence of Mg^{2+} have only shown full closure events, without evidence for partial closure to subconducting states (Matsuda et al., 1987; Matsuda, 1988; Taglialatela, Wible, Caporaso, and Brown, 1994; Wible et al., 1994). A modification to model IIIb, in which all three blocking reactions are concentration dependent, could describe a mechanism where each of three barrels is blocked separately but *dependently* by a single polyamine molecule. If blocking a first barrel could sufficiently enhance the rate of block of other channels, then single channel records might appear to show only full amplitude closure.[6] However, with the limited availability of evidence for 1/3 subconductance states in inward rectifiers in general (Matsuda, 1988; Matsuda et al., 1989), and thus far no evidence for such states in cloned channels, such a model seems unnecessarily complex, and the "long-pore plugging" model may be more realistic.

CONCLUSIONS

The results presented above strongly argue that time-dependent rectification of the strong inward rectifiers HRK1 and IRK1 results from channel block by cytoplasmic polyamines (spermine and spermidine) and not from an intrinsic gating of the channel protein. The results suggest that these polyamines, with an additional contribution by putrescine and Mg^{2+} ions, cause classical strong inward, or anomalous, rectification by a steeply voltage-dependent plugging of the channel pore, and that relief of this plugging at negative voltages is the activation process in strong inward rectifier K^+ channels. It is likely that rectification and time-dependent gating of other K^+ channels also result from channel block by polyamines. Cellular concentrations of polyamines, and hence the degree of rectification of K^+ channels,

6. As the cooperativity resulting from block of the first barrel is increased, so that the second and third blocking rates approach instantaneous, the model reduces to a simple two-state model (O = B), since there is no residence time in intermediate states (2/3O, 1/3O), i.e., as soon as 2/3O is reached, the other two barrels block. As discussed above, such a simple model (model I) cannot account for the data.

might be regulated, providing cells with a novel means of modulating their own excitability.

APPENDIX

Model IIa is described by individual reaction rates as follows:

$$[\alpha] = \alpha_0 \cdot [SP] \qquad \beta = \beta_0 \cdot \exp(-V_M \cdot \lambda_\beta)$$
$$\gamma = \gamma_0 \cdot \exp(-V_M \cdot \lambda_\gamma) \quad \delta = \delta_0 \cdot \exp(-V_M \cdot \lambda_\delta), \tag{A1}$$

where λ_i is the voltage sensitivity of a given rate constant (i) and α_0, β_0, γ_0, and δ_0 are rate constants at zero membrane potential, and [SP] is the concentration of spermine.

From the individual rate constants, two equilibrium constants, K_1 and K_2, can be written as follows:

$$K_1(V_M) = \exp([-(V_M - V_{1/2}{}^1)] \cdot \lambda_\beta K_2(V_M) = \exp([-(V_M - V_{1/2}{}^2)] \cdot (\lambda_\gamma + \lambda_\delta), \tag{A2}$$

where $V_{1/2}{}^i$ is the membrane potential at which "on" and "off" rates for each transition are equal to each other [$\alpha_o \cdot [SP] = \beta(V_M)$ and $\gamma(V_M) = \delta(V_M)$]. It is important to note here that $V_{1/2}{}^i$ is a function of α_0, β_0, β_0 and δ_0 and can be represented in the following forms:

$$V_{1/2}{}^1 = -\log_e(\alpha_0/\beta_0)/\lambda_\beta \qquad V_{1/2}{}^2 = -\log_e(\gamma_0/\delta_0)/(\lambda_\gamma + \lambda_\delta). \tag{A3}$$

From Eqs A1 and A2, the voltage sensitivity of the equilibrium rate constant, λ_i, can be expressed as the effective valency Z_i, which is the number of elementary charges (n) of a blocking particle taking part in each transition multiplied by the "electrical distance" Δ (expressed as a fraction of the electrical field) passed during this transition:

$$Z = n \cdot \Delta \qquad Z_i = \lambda_i \cdot R \cdot T/F, \tag{A4}$$

where R, T, and F have their usual meaning.

Models IIb and IIIa are described by similar equations, with the following difference:

$$[\gamma] = \gamma_0 \cdot [SP]. \tag{A5}$$

Model IIIb contains a similar set of individual reactions, plus additional voltage-dependent transitions between states B_2 and B_3 described as follows:

$$\omega = \omega_0 \cdot \exp(V_M \cdot \lambda_\omega) \qquad \epsilon = \epsilon_0 \cdot \exp(-V_M \cdot \lambda_\epsilon). \tag{A6}$$

The mechanistically complete scheme (Fig. 11) requires an additional state B_4 with rate constants [γ^*], δ^*, ω^*, and ϵ^* analogous to those described above.

We thank Paul Schlesinger for useful discussions. IRK1 was a gift from Lou Philipson and Dorothy Hanck (University of Chicago).

The work was supported by grants 193169 from the Juvenile Diabetes Foundation International and HL45742 and HL54171 from the National Institutes of Health (C. G. Nichols), fellowships from the McDonnell Neuroscience Foundation (E. Makhina) and the American Heart Association, Missouri Affiliate (A. N. Lopatin), and an Established Investigatorship from the American Heart Association (C. G. Nichols).

Original version received 9 January 1995 and accepted version received 10 May 1995.

REFERENCES

Armstrong, C. M. 1969. Inactivation of the potassium conductance and related phenomena caused by quaternary ammonium ion injected into squid axons. *Journal of General Physiology.* 54:553–575.

Bachrach, U. 1973. *Function of Naturally Occurring Polyamines.* Academic Press, New York.

Bartolome, J., J. Huguenard, and T. A. Slotkin 1980. Role of ornithine decarboxylase in cardiac growth and hypertrophy *Science.* 210:749–790.

Basu, H. S., M. Pellarin, B. G. Feuerstein, A. Shirahata, K. Samejima, D. F. Deen, and L. J. Marton. 1993. Interaction of a polyamine analogue, 1,19-bis-(ethylamino)-5,10,15-triazanonadecane, BE-4-4-4-4), with DNA and effect on growth, survival, and polyamine levels in seven human brain tumor cell lines. *Cancer Research.* 53:3948–3955.

Brew, H., P. T. A. Gray, P. Mobbs, and D. Attwell. 1986. Endfeet of retinal glial cells have higher densities of ion channels that mediate K^+ buffering. *Nature.* 324:486–488.

Brismar, T., and V. P. Collins. 1989. Inwardly rectifying potassium channels in human malignant glioma cells. *Brain Research.* 480:249–258.

Burton, F. L., and O. F. Hutter. 1990. Sensitivity to flow of intrinsic gating in inwardly rectifying potassium channel from mammalian skeletal muscle. *Journal of Physiology.* 424:253–261.

Caldarera, C. M., G. Orlandini, A. Casti, and G. J. Moruzzi. 1974. Polyamine and nucleic acid metabolism in myocardial hypertrophy of the overloaded heart. *Molecular and Cellular Cardiology.* 6:95–104.

Carmeliet, E. 1982. Induction and removal of inward-going rectification in sheep Purkinje fibres. *Journal of Physiology.* 327:285–308.

Cohen, I. S., D. DiFrancesco, N. K. Mulrine, and P. Pennefather. 1989. Internal and external K^+ help gate the inward rectifier. *Biophysical Journal.* 55:197–202.

Constanti, A., and M. Galvan. 1983. Fast inward-rectifying current accounts for anomalous rectification in olfactory cortex neurones. *Journal of Physiology.* 335:153–178.

Feuerstein, B.G., J. Szollozi, H. S. Basu, and L. J. Marton. 1992. alpha-Difluoromethylornithine alters calcium signaling in platelet-derived growth factor-stimulated A172 brain tumor cells in culture. *Cancer Research.* 52:6782–6789.

Ficker, E., M. Taglialatela, B. A. Wible, C. M. Henley, and A. M. Brown. 1994. Spermine and spermidine as gating molecules for inward rectifier K^+ channels. *Science.* 266:1068–1072.

Hagiwara, S., and K. Takahashi. 1974. The anomalous rectification and cation selectivity of the membrane of a starfish egg. *Journal of Membrane Biology.* 18:61–80.

Hagiwara, S., S. Miyazaki, and N. P. Rosenthal. 1976. Potassium current and the effect of cesium on this current during anomalous rectification of the egg cell membrane of a starfish. *Journal of General Physiology.* 67:621–638.

Hayashi, Y., Y. Hattori, A. Moriwaki, Y. F. Lu, and Y. Hori. 1993. Increases in brain polyamine concentrations in chemical kindling and single convulsion induced by pentylenetetrazol in rats. *Neuroscience Letters.* 149:63–66.

Hestrin, S. 1987. The properties and function of inward rectification in rod photoreceptors of the tiger salamander. *Journal of Physiology.* 390:319–333.

Hille, B. 1992. *Ionic Channels of Excitable Membranes.* Sinauer Associates Inc., Sunderland, MA.

Hille, B., and W. Schwartz. 1978. Potassium channels as multi-ion, single-file pores. *Journal of General Physiology.* 72:409–442.

Inoue, M., S. Nakajima, and Y. Nakajima. 1988. Somatostatin induces an inward rectification in rat locus coeruleus neurones through a pertussis toxin-sensitive mechanism. *Journal of Physiology.* 407: 177–198.

Ishihara, K., and M. Hiraoka. 1994. Gating mechanisms of the cloned inward rectifier potassium channel from mouse heart. *Journal of Membrane Biology.* 142:55–64.

Ishihara, K., A. Mitsuiye, A. Noma, and M. Takano. 1989. The Mg^{2+} block and intrinsic gating underlying inward rectification of the K^+ current in guinea-pig cardiac myocytes. *Journal of Physiology.* 419:297–320.

Kandel, E., and L. Tauc. 1966. Anomalous rectification in the metacerebral giant cells and its consequences for synaptic transmission. *Journal of Physiology.* 183:287–304.

Katz, B. 1949. Les constantes electriques de la membrane du muscle. *Archives de Science et Physiologie.* 2:285–299.

Kubo, Y., T. J. Baldwin, Y. N. Jan, and L. Y. Jan. 1993. Primary structure and functional expression of a mouse inward rectifier potassium channel. *Nature.* 362:127–133.

Kurachi, Y. 1985. Voltage-dependent activation of the inward rectifier potassium channel in the ventricular cell membrane of guinea-pig heart. *Journal of Physiology.* 366:365–385.

Laschet, J., S. Trottier, T. Grisar, and V. Leviel. 1992. Polyamine metabolism in epileptic cortex. *Epilepsy Research.* 12:151–156.

Leech, C. A., and P. R. Stanfield. 1981. Inward rectification in frog skeletal muscle fibres and its dependence of membrane potential and external potassium. *Journal of Physiology.* 319:295–309.

Liman, E. R., P. Hess, F. Weaver, and G. Koren. 1991. Voltage-sensing residues in the S4 region of a mammalian K^+ channel. *Nature.* 353:752–756.

Lopatin, A. N., E. N. Makhina, and C. G. Nichols. 1994. Potassium channel block by cytoplasmic polyamines as the mechanism of intrinsic rectification. *Nature.* 372:366–369.

Lopez, G. A., Y. N. Jan, and L. Y. Jan. 1991. Hydrophobic substitution mutations in the S4 sequence alter voltage-dependent gating in *Shaker* K^+ channels. *Proceedings of the National Academy of Sciences, USA.* 88:2931–2935.

Lu, Z., and R. MacKinnon. 1994. Electrostatic tuning of Mg^{2+} affinity in an inward rectifier K^+ channel. *Nature.* 371:243–246.

Makhina, E. N., A. J. Kelly, A. N. Lopatin, R. W. Mercer., and C. G. Nichols. 1994. Cloning and expression of a novel inward rectifier potassium channel from human brain. *Journal of Biological Chemistry.* 269:20468–20474.

Matsuda, H. 1988. Open-state substructure of inwardly rectifying potassium channels revealed by magnesium block in guinea-pig heart cells. *Journal of Physiology.* 397:237–258.

Matsuda, H., H. Matsuura, and A. Noma. 1989. Triple-barrel structure of inwardly rectifying K^+ channels revealed by Cs^+ and Rb^+ block in guinea-pig heart cells. *Journal of Physiology.* 413:139–157.

Matsuda, H., A. Saigusa, and H. Irisawa. 1987. Ohmic conductance through the inwardly rectifying K^+ channel and blocking by internal Mg^{2+}. *Nature.* 325:156–159.

Mialon, P., C. Cann-Moisan, L. Barthelemy, J. Caroff, P. Joanny, and J. Steinberg. 1993. Effect of one hyperbaric oxygen-induced convulsion on cortical polyamine content in two strains of mice. *Neuroscience Letters.* 160:1–3.

Miledi, R., and I. Parker. 1984. Chloride current induced by injection of calcium into *Xenopus* oocytes. *Journal of Physiology.* 357:173–183.

Newman, E. A. 1985. Regulation of potassium levels by glial cells in the retina. *Trends in Neuroscience.* 8:156–159.

Newman, E. A. 1993. Inward-rectifying potassium channels in retinal glial (Muller) cells. *Journal of*

Neuroscience. 13:3333–3345.

Noble, D. 1965. Electrical properties of cardiac muscle attributable to inward going (anomalous) rectification. *Journal of Cellular and Comparative Physiology.* 66:127–136.

Oliva, C., I. S. Cohen, and P. Pennefather. 1990. The mechanism of rectification of I_{K1} in canine Purkinje myocytes. *Journal of General Physiology.* 96:299–318.

Osborne, H. B., O. Mulner-Lorillon, J. Marot, and R. Belle. 1989. Polyamine levels during Xenopus laevis oogenesis: a role in oocyte competence to meiotic resumption. *Biochemical and Biophysical Research Communications.* 158:520–526.

Pegg, A. E., and P. P. McCann. 1980. Polyamine metabolism and function. *American Journal of Physiology.* 243:C212–C221.

Pennefather, P. S., and T. E. De Coursey. 1994. A scheme to account for the effects of Rb^+ and K^+ on inward rectifier K channels of bovine artery endothelial cells. *Journal of General Physiology.* 103:549–581.

Pennefather, P., C. Oliva, and N. K. Mulrine. 1992. Origin of the potassium and voltage dependence of the cardiac inwardly rectifying K-current (I_{K1}). *Biophysical Journal.* 61:448–462.

Perier, F., C. M. Radeke, and C. A. Vandenberg. 1994. Primary sequence and characterization of a human hippocampal inwardly rectifying potassium channel, HIR. *Proceedings of the National Academy of Sciences, USA.* 91:6240–6244.

Reynolds, I. J., 1992. Interactions between zinc and spermidine on the N-methyl-D-aspartate receptor complex: clues to the mechanism of action of 1,10-*bis* (guanidino) decane and pentamidine. *Journal of Pharmacology and Experimental Therapeutics.* 263:632–638.

Romano, C., and K. Williams. 1994. Ch.4. Modulation of NMDA receptors by polyamines. *In The Neuropharmacology of Polyamines.* C. Carter, editor. Academic Press, New York. Ch. 4.

Saigusa, A., and H. Matsuda. 1988. Outward currents through the inwardly rectifying potassium channel of guinea-pig ventricular cells. *Japanese Journal of Physiology.* 38:77–91.

Scott, R. H., K. G. Sutton, and A. C. Dolphin. 1993. Interactions of polyamines with neuronal ion channels. *Trends in Neuroscience.* 16:153–160.

Seiler, N. 1994. Formation, catabolism and properties of the natural polyamines. *In The Neuropharmacology of Polyamines.* C. Carter, editor. Academic Press, New York. Ch. 1.

Shaw, G. G. 1994. Polyamines as neurotransmitters or modulators. *In* The Neuropharmacology of Polyamines. C. Carter, editor. Academic Press, New York. Ch. 3.

Silver, M. R., and T. E. DeCoursey. 1990. Intrinsic gating of inward rectifier in bovine pulmonary artery endothelial cells in the presence or absence of internal Mg^{2+}. *Journal of General Physiology.* 96: 109–133.

Silver, M. R., M. S. Shapiro, and T. E. DeCoursey. 1994. Effects of external Rb^+ on inward rectifier K^+ channels of bovine pulmonary artery endothelial cells. *Journal of General Physiology.* 103:519–548.

Stanfield, P. R., N. W. Davies, P. A. Shelton, I. A. Khan, W. J. Brammar, N. B. Standen, and E. C. Conley. 1994a. The intrinsic gating of inward rectifier K^+ channels expressed from the murine IRK1 gene depends on voltage, K^+ and Mg^{2+}. *Journal of Physiology.* 475:1–4.

Stanfield, P. R., N. W. Davies, P. A. Shelton, M. J. Sutcliffe, I. A. Khan, W. J. Brammar, and E. C. Conley. 1994b. A single aspartate residue is involved in both intrinsic gating and blockage by Mg^{2+} of the inward rectifier. *Journal of Physiology.* 478:1–6.

Stanfield, P. R., N. B. Standen, C. A. Leech, and F. M. Ashcroft. 1981. Inward rectification in skeletal muscle fibres. *Advances in Physiological Sciences.* 5:247–262.

Tabor, C. W., and H. Tabor. 1984. Polyamines. *Annual Review of Biochemistry.* 53:749–790.

Taglialatela, M., B. A. Wible, R. Caporaso, and A. M. Brown. 1994. Specification of pore properties by the carboxyl terminus of inwardly rectifying K^+ channels. *Science.* 264:844–847.

Tourneur, Y., R. Mitra, M. Morad, and O. Rougier. 1987. Activation properties of the inward-rectify-

ing potassium channel in mammalian cells. *Journal of Membrane Biology.* 97:127–135.

Vandenberg, C. A. 1987. Inward rectification of a potassium channel in cardiac ventricular cells depends on internal magnesium ions. *Proceedings of the National Academy of Sciences, USA.* 84:2560–2562.

van Leeuwenhoek, A. 1678. Observationes D. Anthonii Leeuwenhoek, de natis e semine genitali animalculis. *Philosophical Transactions of the Royal Society.* 12:1040–1043.

Weidmann, S. 1951. Effect of current flow on the membrane potential of cardiac muscle. *Journal of Physiology.* 115:227–236.

Wible, B. A., M. Taglialatela, E. Ficker, and A. M. Brown. 1994. Gating of inwardly rectifying K^+ channels localized to a single negatively charged residue. *Nature.* 371:246–249.

Williams, J. T., W. F. Colmers, and Z. Z. Pan. 1988. Voltage- and ligand-activated inwardly rectifying currents in dorsal raphe neurons *in vitro*. *Journal of Neuroscience.* 8:3499–3506.

Williams, K., C. Romano, M. A. Dichter, and P. B. Molinoff. 1991. Minireview: Modulation of the NMDA receptor by polyamines. *Life Sciences.* 48:469–498.

Woodhull, A. M. 1973. Ionic blockage of sodium channels in nerve. *Journal of General Physiology.* 61: 687–708.